Past and future radial growth and water-use efficiency of Fagus sylvatica and Quercus robur in a long-term climate refugium

Didier Bert, François F. Lebourgeois, Adib Ouayjan, Alexis Ducousso, Jérôme Ogée, Arndt Hampe

The final version of the paper can be found at :https://doi.org/10.1016/j.dendro.2022.125939
Dendrochronologia, 72, April 2022, 125939

Past and future radial growth and water-use efficiency of *Fagus sylvatica* and *Quercus robur* in a long-term climate refugium

Didier Bert[a*], François Lebourgeois[b], Adib Ouayjan[a], Alexis Ducousso[a], Jérôme Ogée[c], Arndt Hampe[a]

[a] BioGeCo, INRAE, University of Bordeaux, F-33610 Cestas, France

[b] Université de Lorraine, AgroParisTech, INRAE, Silva, F-54000 Nancy, France

[c] ISPA, INRAE, F-33140 Villenave d'Ornon, France

Email: didier.bert@inrae.fr

* Author for correspondence

ABSTRACT

The low-latitudinal range margins of many temperate and boreal tree species consist of scattered populations that persist locally in climate refugia. Recent studies have shown that such populations can be remarkably resilient, yet their past resilience does not imply that they are immune to threats from future climate change. Hence, the functioning of refugial tree populations needs to be better understood for properly anticipating their prospects. We performed a detailed study of tree radial growth and vigour in a long-term climate refugial population of beech (*Fagus sylvatica*) and compared the observed trends with those of co-occurring pedunculate oak (*Quercus robur*). Annual growth rates (BAI) of both species were similar to those observed in range-core populations, but natural lifespan was half than in mountains. The master chronologies spanning 1870 to 2015 revealed a 22 % (*Fagus*) and 20 % (*Quercus*) increase in BAI up to the 1980s and a slighter decrease (-6 % for *Fagus*, -9 % for *Quercus*) since then. Stable carbon isotope measurements ($\delta^{13}C$) revealed no effect of cambial age and an increase of water-use efficiency (iWUE) from 1870 to 2015 of ca. 50 % (*Fagus*) and 20 % (*Quercus*). The trend continued until 2015 in *Fagus*, whereas *Quercus* reached its maximum in the 1980s. A detailed analysis of climate-annual growth relationships based on a 118-year meterological record revealed a major role of water availability in the current and previous year. We used the observed climatic relationships to model future growth trends until 2100 for the IPCC scenarios RCP4.5 and RCP8.5. Most projections revealed no changes in current growth rates, suggesting that this climate refugium will be able to provide suitable conditions for the persistence of *Fagus* and *Quercus* over the coming decades even under a warmer and drier regional climate. Overall, our study provides valuable insights into the precise climatic and biological mechanisms that contribute to enhance the persistence of refugial tree populations under ongoing climate change.

Keywords

Tree ring, Interglacial refugium, *Fagus sylvatica, Quercus robur,* Growth trends, Carbon isotopes

1. INTRODUCTION

The impact of increasing temperatures and more severe and frequent droughts as a consequence of global climate change has already affected many biomes (Parmesan, 2006; Allen et al., 2010; Taccoen et al., 2019) and has drawn considerable attention to the fate of trees and forests (Badeau et al., 1996; Millar et al., 2007; Petit et al., 2008; Lindner et al., 2010; Jump et al., 2017). There is great concern that modern climate warming could outpace the response capacity of many tree populations (Jump et al., 2009). Tree populations growing near the low-latitude limits of species ranges are commonly assumed to be particularly at risk from climate change. However, such populations occur often within areas of high habitat heterogeneity where local environmental conditions have allowed populations to persist despite regionally unfavourable climate, so-called climate refugia (Hampe and Jump, 2011). Such a decoupling between local and regional climate can arise as consequence of topography, smaller-scale terrain effects, edaphic particularities, or vegetation structure (Dobrowski, 2011). Some dendrochronological surveys have shown that refugial tree populations can actually be more resilient to modern climate change than those at higher latitudes (Cavin and Jump 2016; Vilà-Cabrera and Jump 2019). However, the past survival of tree populations in climate refugia does not imply that they are immune to threats from modern climate change (Sanchez-Salgueiro et al. 2017; Dorado-Liñan et al. 2018). Hence, further studies are required to understand the functioning of refugial tree populations and to anticipate their responses to anthropogenic climate warming (Vilà-Cabrera and Jump 2019).

European beech (*Fagus sylvatica* L., hereafter referred to as *Fagus*) is one of the major broadleaf forest trees in Europe and one of the most successful plant species in central Europe (Willner at al., 2017). It grows in a wide range of edaphic and climatic conditions and tends to form mono-specific stands in large parts of its distribution range (Peters, 1997). It is not constrained by soil acidity, soil nutrition or humus type, but tends to avoid sites with very dry soils or with flooding or high groundwater levels (Peters, 1997). The species is thus sensitive to edaphic and atmospheric drought, which can be exacerbated by high air temperatures (Lebourgeois et al., 2005; Piedallu et al., 2009). Therefore, in the southern part of its range, especially in lowland forests, climate-based projections suggest that *Fagus* could be adversely affected by future climate change (Geßler et al., 2007; Meier et al. 2011; Cheaib et al, 2012; Charru et al., 2017). The negative impacts of climate change on the growth of marginal populations have been recorded where beech is putatively least adapted to its environment, i.e. at low elevation in Spain (Jump et al., 2006) and in Italy (Piovesan et al., 2008). At these locations, warming temperatures not compensated by higher precipitation increased drought stress. On the other hand, Cavin and Jump (2016) showed that southern beech populations may be relatively resistant to climate warming as they typically grow in areas with particularly favourable and stable microclimates (i.e., climate refugia).

Tree radial increment is a well-proven quantitative proxy to investigate spatial and temporal changes in tree vitality, and highlight the effects of natural and anthropogenic factors on tree growth (Bert, 1993; Badeau et al., 1996; Gillner et al., 2013; Bachtobji Bouachir et al., 2017; Cailleret et al., 2016; Cavin and Jump, 2016; Preisler et al., 2019). However, tree growth is the result of many biological processes that respond strongly but differently to climate events such as droughts. Also, the impact of drought on tree growth can be partly compensated by increasing atmospheric CO_2 concentrations that stimulate photosynthesis and reduce plant water loss. This higher water-use efficiency of plants (defined as the ratio of photosynthesis to transpiration) is also recorded in tree rings, as it is strongly related to the carbon isotope ratio ($^{13}C/^{12}C$) of wood cellulose (Farquhar and Richards, 1984; Bert et al., 1997; Hughes, 2000; Keenan et al., 2013). These annual records of plant water-use efficiency provide a means to study past variations of the drought response of trees (Leavitt and Long, 1989; Bert et al., 1997; Duquesnay et al., 1998; Waterhouse et al., 2004; Peñuelas et al., 2011; Frank et al., 2015).

In the present study, we performed a 150-yr-long reconstruction of radial growth and water use efficiency of a *Fagus* refugial population located along a riparian corridor where local conditions and landscape heterogeneity buffer the effect of ongoing climate warming. An important particularity of this population is the fact that its growing site already harboured *Fagus* during the last Quaternary glacial period (De Lafontaine et al., 2014), suggesting that the area has served as long-term refugium for the species both under the cold-dry conditions of the late Quaternary as well as under the warm-dry regional climate of our times. We compared trends observed in *Fagus* with those of *Quercus robur* L. (referred to as *Quercus* hereafter) trees co-occurring the same riparian forest. The particularity of this study system makes it an instructive model for studying how marginal populations within climate refugia could respond to increasing temperature. For this purpose, we identified the main climate factors that drove the growth patterns, and used these relationships to make projections of the future evolution of tree growth based on climate change scenarios. The aims were: 1. to examine the dynamics of growth and water-use efficiency over the last 150 years in order to estimate the vitality of the two species in the climate refugia; 2. to link the climate factors to the growth in order to project the future evolution of growth based on climate change scenarios; 3. to compare the response of this refugial population situated near the species' range margin to that of range-core populations.

2. MATERIALS AND METHODS

1.1. Study site and species

The study was conducted in a valley 55 km south of Bordeaux, France, within a riparian corridor spread linearly over 7 km on the banks of the Ciron river (Fig.1, 44°22 '52"N, 0°15'25"W). This riparian forest is limited to the slopes of a karstic canyon along the river with a maximal altitude around 30 m above the river (i.e. about 50 m above sea level). This site is ecologically atypical for *Fagus* because this species usually prefers well-drained soils and does not tolerate excess water (Packham et al., 2012). Yet the area harbours the largest lowland population of this species in SW France (Timbal and Ducousso, 2010) with slightly less than 1000 adult trees (Ouayjan and Hampe, 2018). Interestingly, fossil charcoal records and genetic data indicate that the precise place where *Fagus* persists today within its interglacial climate refugium already served as a climate refugium for *Fagus* during the last glacial period (De Lafontaine et al., 2013, 2014). The current beech population is likely to represent a remainder of this former population. It builds a mixed broadleaf forest together with other mesic species such as Pedunculate oak (*Quercus robur*), alder (*Alnus glutinosa*), small-leaved lime (*Tilia cordata*), ash (*Fraxinus excelsior*), and hazel (*Corylus avellana*), among others. Pedunculate oak is one of the most dominant accompanying forest tree species and is therefore a good candidate for studying inter-specific growth patterns under the same environmental conditions.

The region's climate is characterised by humid and mild winters and dry summers with a deficit in water balance occurring from the beginning of May to the end of September (Fig.S1). Daily climate data were retrieved from the INRAE CLIMATIK database and come from a weather station located in Sauternes (44°32'39"N, 0°19'45"W, ca. 20 km north of the study site). These data cover a period from 1897 to 2015 during which the temperature showed a significant increase for half of the year, while precipitation trends were weak and not significant (Fig.S2 and Table S1). At these latitudes, *Fagus* usually thrives in mountain ranges with mean annual temperature below 10.5°C, whereas the region around the Ciron has a temperature of about 13°C, and even almost 14°C since the 2000s. The average annual precipitation is 812 mm (sd = 145 mm).

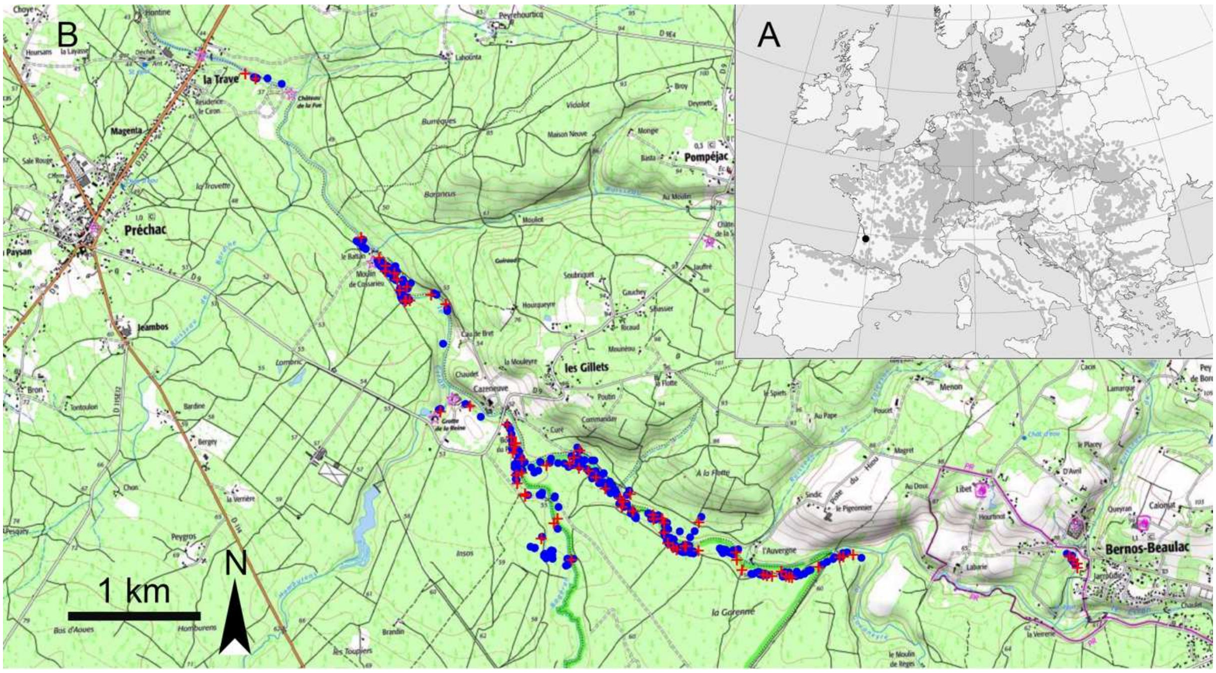

Figure 1. Study area and tree sampling. A. Geographical range of *Fagus sylvatica* (in grey) and location of the study area in SW France (black dot). B. Study area with the cored trees of *Fagus* (n = 319, blue dots) and *Quercus* (n = 79, red crosses). Their narrow distribution along the Ciron river pinpoints the function of its gorges as long-term climate refugium for the species. Maps adapted by the authors from Geoportail and Euforgen under Creative Commons Corporation license.

2.1. Tree-ring chronologies

A field campaign was carried out at the end of 2015 to resample 294 out of the 932 adult beech trees identified during an exhaustive sampling for a genotypic characterisation of the population (Ouayjan and Hampe, 2018), plus an additional sample of 25 sub-adult trees. Based on detailed previous field observations of seed production (A. Hampe, unpublished data), we used a threshold value of 70 cm in circumference at breast height (1.3 m above ground) to separate adult and sub-adult trees. In addition, 79 *Quercus* were sampled within the study site. One wood core was taken per tree at breast height using a 5 mm diameter increment borer.

In the laboratory, wood cores were flattened with a blade and prepared using standard dendrochronology methods following Phipps (1985). Cores were scanned at 1200 dpi and tree-ring width was measured using WinDENDRO version 2012 (Regent Instruments Inc.). The mean curve of tree-ring width as a function of years was calculated for each species and used in WinDENDRO for cross-dating. This step allowed to assign to each tree ring its actual year of formation by using some pointer years of high or low growth. Pointer years were calculated from the raw data of crossdated tree-ring widths using the function dendro in the dplR package (Becker, 1989; Bunn, 2008; Mérian, 2012) in R version 3.3.1 (R Development Core Team, 2016). A pointer year was defined with two conditions: (1) the mean growth was at least 10 % lower or higher than during the previous year, (2) at least 75 % of the trees showed the same change in direction. Then, tree-ring widths (in mm) were converted into basal area increments (BAI, in cm^2), to represents tree growth in terms of annual ring area produced. BAI was calculated using the bai.in function in the dplR package considering the distance to the pith estimated with a template of concentric circles when coring missed the innermost tree-ring.

As BAI evolves from pith to bark over tree ageing, the comparison of raw BAI of young and old rings at a given year is meanlingless (Cook and Kairiukstis, 1990). It is therefore necessary to standardize BAI in order to remove this age trend using the regional curve standardization (RCS) method (Becker, 1989; Esper et al., 2003; Briffa & Melvin, 2011). For that, the BAI of each tree ring, whose age from pith is known, was transformed into a percentage of the mean BAI of all the tree rings of the same age. As the raw mean curve of BAI according to tree-ring age presented some random variations, each chronology was detrended using a smooth curve made of two fitted functions. The increasing part of the chronology (i.e. until 77-yr-old for *Fagus* and 51yr-old for *Quercus*) was fitted by a polynomial function, determined by a progressive multiple stepwise regression, and the decreasing part (i.e. after 77 yr-old and 51 yr-old for *Fagus* and *Quercus*, respectively) was fitted using used an exponential function (Fig.2). The equation of the selected function allowed to convert BAI (cm^2) to growth indices (GI, in %) for both target species:

$$GI_n = 100 \times BAI_n / BAI_{model}$$

where BAI_n is the BAI for cambial age *n*, and BAI_{model} is the value of the fitted curve for the same cambial age. After the standardization, the calculation of the mean of all GI available at each year produced the master chronologies for *Fagus* and *Quercus*.

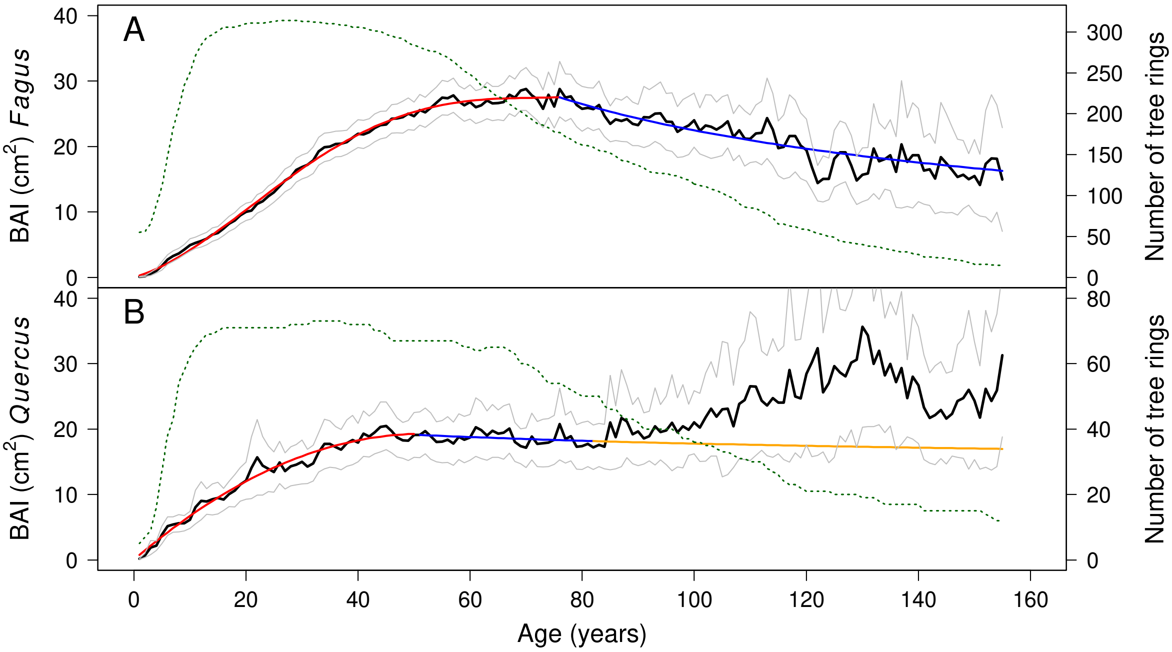

Figure 2. BAI timeseries and fitted curves used to standardize tree-ring widths into a Growth Index. For both species, the dotted curve gives the number of tree rings per year of age. The black curve represents the average BAI (cm^2) as function of cambial age and the grey area is the 95 % confidence interval for the mean. **A**. For *Fagus*, the red line displays a polynomial function: $BAI_{model} = 2.404\ 10^{-1}\ Age + 2.178\ 10^{-2}\ Age^2 - 4.526\ 10^{-4}\ Age^3 + 2.462\ 10^{-6}\ Age^4$. The blue line indicates an exponential function for cambial age greater than 76 years old: $BAI_{model} = e^{6.498 - 0.735 \log(Age)}$. **B.** For *Quercus*, the red line indicates a square function: $BAI_{model} = 0.7431\ Age - 0.007157\ Age^2$. The blue line indicates an exponential function: $BAI_{model} = e^{3.370 - 0.1069 \log(Age)}$. Because the BAI curve fluctuates markedly as soon as the number of rings falls below 35, an extrapolation of the same exponential equation was used for the cambial ages greater than 82 yr-old (orange curve).

Trends in radial growth were characterised using two methods: (1) by analysing the smooth GI timeseries and (2) by analysing the variance of the BAI. For the first approach, the smooth.spline function in stats package in R was used with a spar parameter of 0.9 to display only the long-term trends (Chambers and Hastie, 1992). For the analysis of variance of BAI, cambial age and year plus their interaction were used as fixed factors (Badeau et al., 1995):

$$BAI_{t,a,y} = A_a + Y_y + A_a.Y_y + E_{t,a,y},$$

where $BAI_{t,a,y}$ is the mean basal area increment of tree *t* at cambial age *a* and at year *y*, A_a is the effect of age *a*, Y_y is the effect of year *y*, $A_a.Y_y$ is the interaction between age and year, and $E_{t,a,y}$ is the residual. Taking all tree-rings would lead to very numerous and unbalanced combinations of ages and years. In order to reduce the number of combinations and remove the high and medium frequency signals and keep only the long-term effects, tree-ring ages were grouped into 4 classes and years into 5 periods of 30 years. Parameters of the model were fitted using the *aov* and *Anova* functions in R, that can account for unbalanced numbers of combinations. Least square estimates of marginal means and their confidence interval were computed with the *emmeans* function with the "proportional" option for unbalanced data (emmeans package ver 1.5.0).

3.1. Climate-driven growth models

The effect of climate on interannual and long-term variation of radial growth were analysed in three main steps: (1) identifying the climatic variables significantly correlated with interannual growth, (2) modelling growth with a linear combination of the most correlated climatic variables, and (3) using the model to predict future growth up to the year 2100.

For the first two steps, we used the data from the weather station located 20 km north of the study site. Climate variables were minimal and maximal daily temperature (in °C) and daily total precipitation (in mm). From these data, we derived the following variables: monthly mean temperature (T), monthly precipitation (P), monthly potential evapotranspiration (PET) using the Thornthwaite method (Thornthwaite, 1948, Table S2), and monthly climatic water balance (WB), expressed as P – PET (Lebourgeois and Piedallu, 2005). As the monthly time step is not necessarily the most integrative to link growth and climate, we also combined these climatic variables into bi-monthly to semi-annual variables from January of the previous year to December of the current year.

Correlation analysis between tree growth and interannual climate variation first requires to extract the high frequency signal from the studied chronologies (Fritts 2012). To do so, we standardized the growth and climatic chronologies with cubic splines (Cook and Peters, 1981; Cook and Kairiukstis, 1990) using the *detrend* function in the dplR package (Bunn, 2008). The splines were fitted with 0.50 for the frequency response at a wavelength of 0.67 times the series length (in years). The difference between the spline and the original series produced detrended timeseries for growth and climatic variables. Correlations between the detrended master chronology of *Fagus* or *Quercus* and each of the detrended climatic variables were then reported as bootstrap correlation coefficients (BCC). Each correlation was calculated on 1000 random samplings of 118 years in the period 1898-2015 (1897 provided the data for the previous-year variables corresponding to 1898). BCC was considered significant when zero was not included in the 95 % confidence interval. The high number of years in the climatic data reduced the influence of extreme events that sometimes complicates the estimation of tree responses to climate factors.

We used two approaches to identify the most parsimonious model able to reproduce the observed radial growth variations: (1) a stepwise regression was run using the *step* function in R, based on the AIC (Akaike Information Criterion), We first selected the most climatic variable that was most tightly correlated with GI, then the most correlated after the effect of the first one was accounted for, and so on. On the way, some variables were dropped when they were no longer significant in the tree growth model. This method led to an overparametrized model for each tree species but highlighted the impact of climate during previous and current years on tree growth. (2) We fit another model for each species using only the first two correlated climate variables in order to identify which climate variables and seasons each species is most sensitive to.

These parsimonious tree growth models were also used to explore how tree growth trends may evolve under future climate scenarios. For this, we had to derive a modified version of the growth models, parametrized on the non-detrended master chronology and climate timeseries, because future climate scenarios only predict non-detrended climate timeseries. For the climate scenarios, we used simulations from two regional climate models (RCM) with a 8-km wide grid over France: WRF and ALADIN, available via http://www.drias-climat.fr. For each RCM, two greenhouse gas emission scenarios (RCP4.5 and RCP8.5; IPCC 2014) were investigated. Predictions of daily temperature and precipitation of the two RCMs for the Ciron valley were used to compute PET and the climatic water balance as described above. These climate variables were then also averaged over periods longer than one month and used in the growth model equations to predict growth trends over the period 2007-2100.

4.1. Water-use efficiency

Given the crucial role of water availability for tree growth and survival, we also quantified past changes in tree water-use efficiency (i.e., the ratio of plant carbon gain to water loss) derived from the carbon isotope ratio ($^{13}C/^{12}C$) of wood holo-cellulose (Table S3). This ratio is traditionally expressed as a deviation from an international standard (called VPDB) and expressed in per mil (thus noted $\delta^{13}C$ from hereon). At the leaf level, photosynthetic carbon isotope discrimination (Δ) is primarily related to the ratio of net leaf assimilation to stomatal conductance which defines the so-called *intrinsic* water-use efficiency (iWUE). Leaf assimilation is the net carbon gain for a leaf and stomatal conductance its "intrinsic" water loss for a unit vapour pressure deficit (Farquhar et al., 1982; Ehleringer et al., 1989; Ehleringer et al., 1993). Variations in iWUE are then imprinted in the $\delta^{13}C$ of newly-formed sugars during photosynthesis, and the isotopic signal is mostly conserved during the translocation of sugars to the cambial cell during wood formation (Damesin and Lelarge, 2003). However, because wood is composed of different compounds (mostly cellulose, hemicellulose and lignin) that are deposited at different dates, it is common practice to analyse the $\delta^{13}C$ of a specific compound, in case climate conditions also modify the fraction of different wood compounds from one year to the next. Here, holo-cellulose, deposited early during new xylem cell formation, was chemically purified before isotopic measurements, following standard protocols (Leavitt and Danzer, 1993). For each sample, 1 mg of holo-cellulose was then inserted in a tin capsule and its $\delta^{13}C$ was determined at the INRAE SILVATECH facility (Nancy, France) with an elemental analyser (Vario ISOTOPE cube, Elementar, Hanau, Germany), interfaced with an isotope ratio mass spectrometer (IsoPrime 100, Isoprime Ltd, Cheadle, UK), with a 0.2 ‰ accuracy.

Variations in tree-ring $\delta^{13}C$ were interpreted in terms of changes in iWUE according to Farquhar et al. (1982):

$$\delta^{13}C = \delta_a - 27 + 1.6\,(27 - 4.4)\ \mathrm{iWUE} / C_a,$$

where δ_a and C_a are respectively the $^{13}C/^{12}C$ isotope ratio and the mixing ratio of atmospheric CO_2 at the time of wood formation. C_a was derived from atmospheric CO_2 data recorded in ice cores before 1958 or directly measured at the Mauna Loa atmospheric station from the Scripps CO_2 Program, and available via a web service (http://scrippsco2.ucsd.edu). Published δ_a data were compiled, updated and smoothed with a cubic spline over the period 1800 to 2015 (see Bert et al., 1997).

A specific sampling was performed to disentangle age and year effects on tree-ring $\delta^{13}C$ (Bert et al., 1997, Duquesnay et al., 1998; Brienen et al., 2017). To test the age effect, wood samples of a given age but from different calendar years were separately measured for $\delta^{13}C$ (Briffa and Melvin, 2011), repeating this for 10 age classes from 15-yr-old to 150-yr-old with a 15-yr timestep. Between 8 and 69 samples with BAI values close to the mean growth curve (Fig.2) were selected per age group. To test the year effect, tree rings of a given age (45-yr-old) were sampled for 14 different 10-yr periods (from 1870 to 2010) and analysed separately. Between 6 and 7 wood sections were selected per decade, all with GI close to the mean GI of the same time-period. Finally, the results of the previous age effect study (see below) allowed to pool the samples for both experiments, thus increasing the number of wood sections up to 6-34 (mainly more than 15) per decade. Each wood sample was a group of five successive tree rings (pentad) analysed together in order to minimise year-to-year variations and assemble enough material for the isotope analysis. Hereafter, the age or the year of a pentad corresponds to the central tree ring of the pentad.

For *Fagus*, a total of 333 pentads from 121 trees were collected. The significance of the hypothesis of an age trend was tested by regression fitted to the observed values of $\delta^{13}C$ as a function of age. For *Quercus*, the smaller number of trees did not allow to study the age effect. The year effect was however tested with 45-yr-old wood sections.

3. RESULTS

5.1. Tree ages, among-year variation and long-term evolution of growth

We first determined the age of the trees reached at the end of 2015. Cambial ages spanned 32-205 years for *Fagus* and 47-245 years for *Quercus*. The number of trees steadily decreased with increasing cambial age as expected for unmanaged stands. Dendrochronological parameters were calculated on detrended tree-ring widths; they indicated that the dataset was well cross-dated and the chronology was highly representative of the local populations for both species (Table 1, Fig.S3). The values of crossdating coefficient showed that the interannual variations were not random and the crossdating of series was then validated. Rbar quantifies the mean inter-tree correlation and indicate a strong common climatic forcing; EPS quantifies the degree to which the master chronology expresses the population chronology (Wigley et al., 1984). EPS was very close to unity because the master chronology for each species mirror the population signal.

Table 1. Summary statistics for trees and tree rings. See also Fig.S3 for details.

	Fagus		***Quercus***	
	Mean	**Std dev**	**Mean**	**Std dev**
$\mathbf{n_{Trees}}$	294	NA	79	NA
$\mathbf{n_{Tree\ rings}}$	25,922	NA	7,366	NA
Tree age	99.1	33.7	113.6	45.0
Diameter at breast height (DBH in cm)	46.0	18.1	52.7	20.6
Tree-ring width in mm	2.37	1.56	2.09	1.33
Basal area increment in cm^2	19.50	19.71	18.52	17.94
Crossdating coefficient	0.498	NA	0.597	NA
Rbar	0.283	NA	0.264	NA
Expressed population signal (EPS)	0.981	NA	0.938	NA
Mean sensitivity (ms)	0.289	0.059	0.243	0.030
1st order correlation (Ar1)	0.248	0.125	0.213	0.110

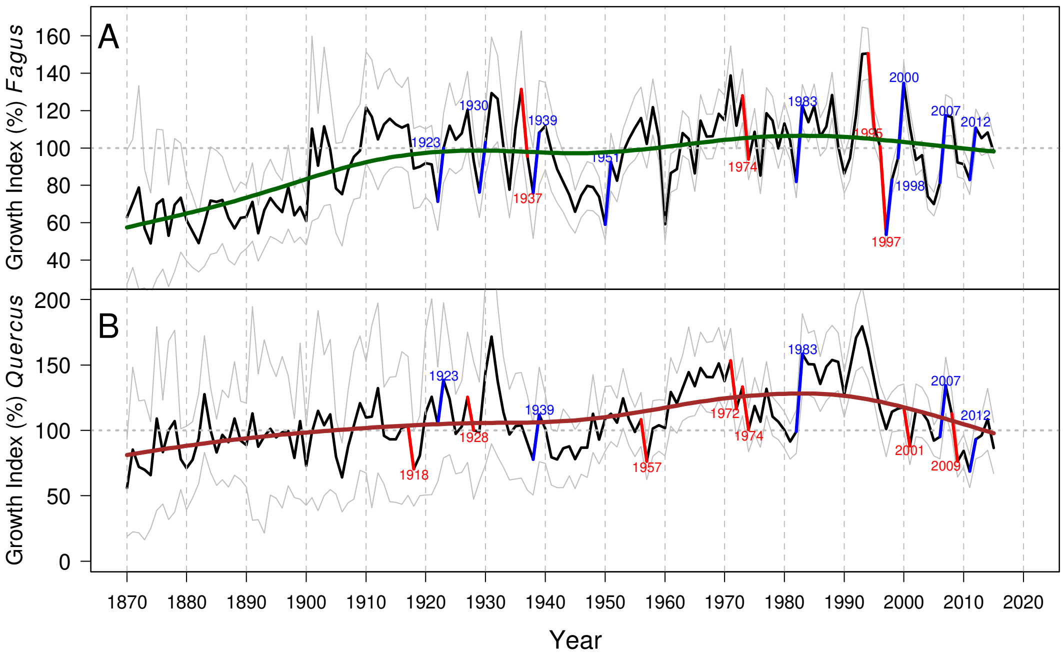

Figure 3. Master chronologies: radial Growth Index in function of year for *Fagus* (A) and *Quercus* (B). The black curve displays the mean, the grey area displays the 95 % confidence interval of the mean, the green or brown lines are smoothing splines to show long-term variations. Pointers years are displayed in red (negative) and blue (positive) lines and dated in the same colour. Number of *Fagus* tree rings in 1870 = 17, in 1880 = 25, 1890 = 37, in 2000 = 294. Number of *Quercus* tree rings in 1870 = 10, in 1880 = 12, 1890 = 17, in 2000 = 79. Note that the Growth Index values on the two graphs cannot be directly compared (see Methods for details of their calculation).

Pointer years for high GI in *Quercus* were all shared with *Fagus* (Fig.3), but *Fagus* had also a few more positive pointer years that were often years with higher-than-normal precipitation during the growing season. Interestingly, pointer years for negative GI in *Fagus* were either drought years (correlation between GI and Water Balance in March to July $r=0.526$, $p<0.0001$) or late frost years (in 1960 and 1997). The smoothed GI curve for *Fagus* showed a strong increase between the 1870s and the 1910s followed by a plateau and a decrease during the 1940s (Fig.3A). From then on, a lower increase occurred until the 1980s followed by a slight decline. The GI curve of *Quercus* followed very similar trends except for the decline after the 1980s that was more pronounced for *Quercus* than for *Fagus*.

Both cambial age and calendar year, as well as their interaction, were highly significant predictors of the variation in BAI (Table 2). The effect of cambial age accounted for the greatest part of the total variance (Fig.2). Calendar year also had a strong influence on BAI, as shown by the smoothing of the GI curves. The significant interaction indicated that the year effect acted differently across the four age classes (not shown). The marginal means were assessed for the 5 periods of years, independent of biological effects related to age (Fig.4). Because the ANOVA was applied to raw data, the means quantify the growth in an absolute scale (BAI in cm^2), which allows to calculate percentages of variation of the growth rate between periods. For *Fagus*, BAI was about 18 cm^2 during the first half of 20th century and increased up to 21.6 cm^2 in the period 1960s to 1980s (+22 %). Then, BAI decreased again to 20.3 cm^2 in the 1990s to 2010s (-6 %). For *Quercus*, the range of mean BAI was similar to beech (17 to 22 cm^2), but the confidence interval were greater owing to the lower number of tree rings. In the long term, BAI increased from 18 cm^2 in 1885 to 19.6 cm^2 in 1915 (+10 %), then decreased to 17 cm^2 in 1945 (-

13 %), increased again to 21.6 cm² in 1975 (+27 %), and finally decreased to 19.6 cm² in 2002 (-9 %). This last lowering was stronger than that of beech (-6 %). These results confirm the variations of growth rate through time shown by the master chronologies.

Table 2. Effect of the cambial age of tree rings and the year of their formation on radial tree growth (BAI) of *Fagus* and *Quercus*. SS, sum of square; df, degree of freedom; F, Fisher's F statistic.

	Fagus				*Quercus*			
	SS	df	*F*	*P*	SS	df	*F*	*P*
Cambial age	962 394	3	954.8	< 0.0001	158 977	3	184.9	< 0.0001
Year	80 150	4	59.6	< 0.0001	28 544	4	24.9	< 0.0001
Interaction	82 493	12	20.5	< 0.0001	67 779	12	19.7	< 0.0001
Residuals	8 619 970	25657			2 066 915	7 211		

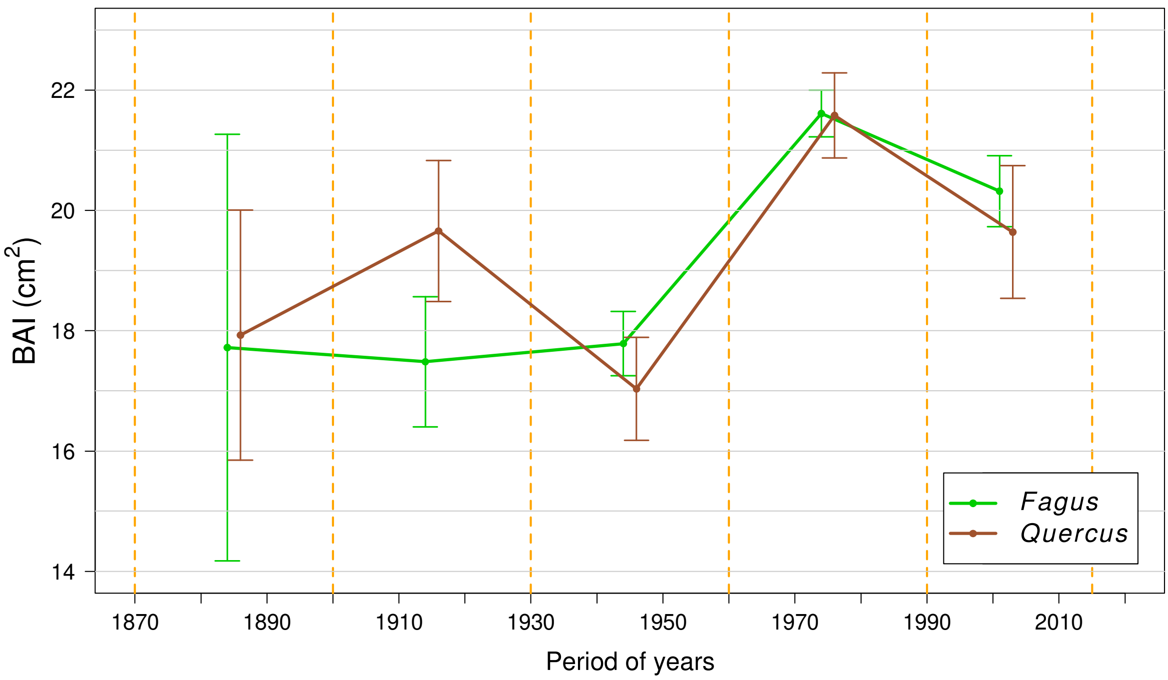

Figure 4. BAI chronologies as a function of calendar year for *Fagus* and *Quercus* populations. Each curve displays the mean BAI by period of 30 years, with the 95 % confidence interval of the mean from the analysis of variance. For *Quercus*, values are slightly shifted on the x-axis for a better display of the confidence intervals.

6.1. Growth and climate

The BCC heatmap showed that previous and current months both significantly influenced radial growth variation (Fig.S4). For *Fagus*, the most correlated variable was the February-to-July climatic water balance (r = 0.579 for WB0207). *Fagus* growth appeared also negatively affected by high growing-season temperature from previous and current years with the strongest negative BCC for June-July temperature (r = -0.314 for T0607). A slightly positive BCC from winter temperature is also indicative of a negative role of low temperatures on *Fagus* growth (r = 0.095 for Tp1102). For *Quercus*, April-to-August precipitation was more closely correlated (r = 0.439 for P0408) than the climatic water balance over the same period (r = 0.389 for WB0408). Temperature was little correlated with growth during the current year (r = 0.043 for T0408), but positively correlated with growth during the previous autumn (r = 0.371 for Tp1011).

In general, climate variables of the previous year were correlated with radial growth but had lower BCC than climate variables of the current year. Some climate variables from the end of the current year showed erratic BCC indicating that tree-ring growth stopped after the end of September. Therefore, variables from current October to December were not used in the following step. For *Fagus*, the most parsimonious model for detrended growth was based on WB0207 and the June-to-September climatic water balance of the previous year (WBp0609):

$$GI_{Fagus} = 0.271\ WBp0609 + 0.613\ WB0207 \qquad \text{(adjusted } R^2\text{=0.424)}$$

Both climate variables were highly significant (p<0.0001). For *Quercus*, the most parsimonious model was based on P0408 and the October-November temperature of the previous year (Tp1011):

$$GI_{Quercus} = 6.352\ Tp1011 + 0.487\ P0408 \quad \text{(adjusted } R^2\text{=0.276)}$$

These growth models were also calibrated using non-detrended time series to perform growth projections using future climate scenarios. The resulting models then became:

$$GI_{Fagus} = 119.237 + 0.286\ WBp0609 + 0.647\ WB0207 \qquad \text{(adjusted } R^2\text{=0.420)}$$

$$GI_{Quercus} = 27.706 + 3.907\ Tp1011 + 0.661\ P0408 \quad \text{(adjusted } R^2\text{=0.205)}$$

Injecting simulated climate data provided by the WRF and Aladin RCMs under emissions scenarios RCP4.5 and RCP8.5 resulted in different trends for the two species (Fig.5). For *Fagus*, the model slightly underestimated the observed trend over the calibration period (1898-2015), and predicted a systematic decrease for the future. However, only the decrease inferred by the Aladin model with RCP8.5 was statistically significant. For *Quercus*, the model also slightly underestimated the observed positive trend over the calibration period, and produced very slight increasing trends for the future growth with only one trend being statistically significant (Aladin model and RCP 4.5 scenario).

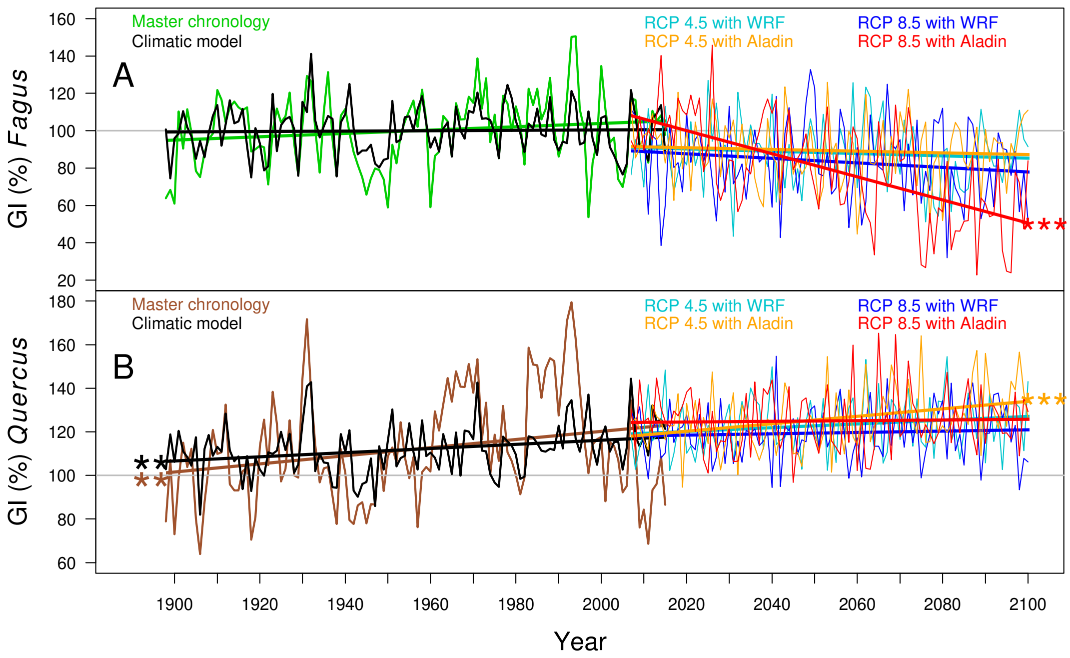

Figure 5. Growth models and future trends. Master chronologies of *Fagus* (green) and *Quercus* (brown), climatic growth models calibrated on the past and used to hindcast past growth (black) and forecast future growth according to climate scenarios (RCP 4.5 and RCP 8.5) and two RCM (WRL and Aladin). Stars indicate significant slopes of the regression (** $p < 0.01$, *** $p < 0.001$).

7.1. Temporal variations in δ^{13}C and iWUE

Our sample for *Fagus* allowed to test for effects of tree age on levels of δ^{13}C in the holocellulose. The simple linear regression of tree-ring δ^{13}C as a function of cambial age showed that there was no significant trend (Table 3, Fig.6). δ^{13}C averaged -26.5‰ (sd = 1.1‰) across 15 to 150 years old tree-rings. The observed lack of age effects on tree-ring $\delta^{13}C$ allowed to pool all wood sections independently of their age and thus to increase the data set for the analysis of year effects.

Table 3. Regression on the effect of age on $\delta^{13}C$ (‰) for *Fagus* in the Ciron valley.

	$\delta^{13}C$			
	Estimate	Std. Error	t value	P
Intercept	-26.617	0.147	-181.3	<0.0001
Age	0.003	0.002	1.18	0.24

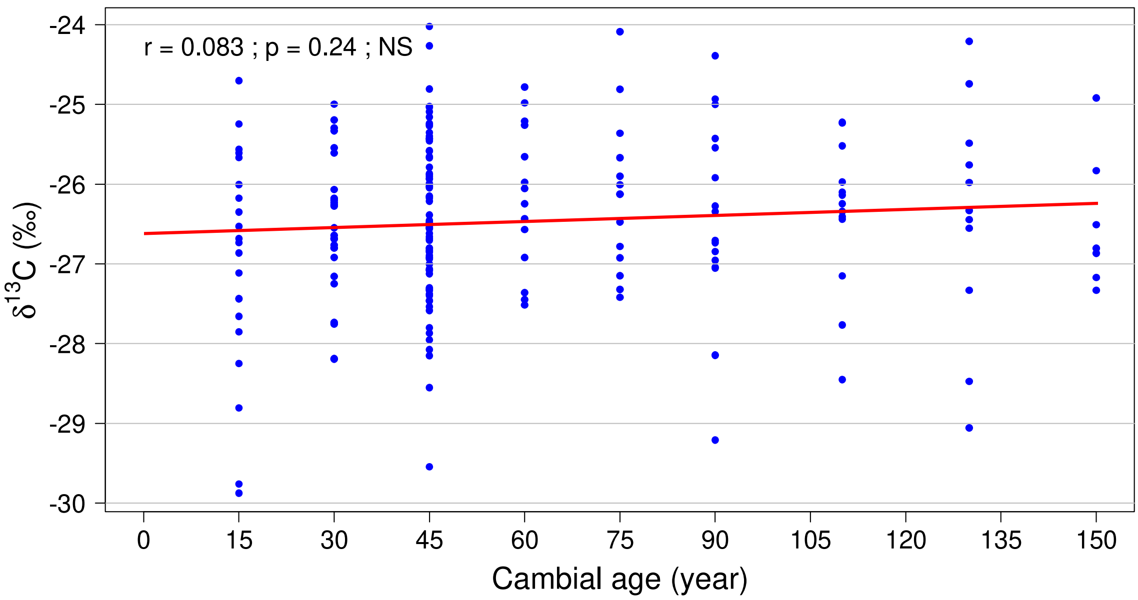

Figure 6. Carbon isotope composition of *Fagus* tree rings ($\delta^{13}C$ in ‰) as function of cambial age (year) in the Ciron valley. Pearson correlation coefficient "r" is also displayed with the probability "p".

The anthropogenic burning of fossil fuel and coal, which originates from plant material naturally depleted in ^{13}C, leads to a decreasing trend in δ_a with a steeper decrease after 1950 (Fig.7A). Such a trend was not completely paralleled by tree-ring $\delta^{13}C$ of *Fagus* and *Quercus* suggesting that photosynthetic discrimination (Δ, defined as δ_a - $\delta^{13}C$) is not constant over time (Fig.7A & 8B). Over the full time period, we found a significant negative correlation between Δ and calendar year for *Fagus* (r = -0.294, $p < 0.0001$) but not for *Quercus* (r = 0.045, p = 0.28). Between 1870 and 2015, intrinsic water-use efficiency (iWUE) increased by ca. 50% for *Fagus* (r = 0.608, $p < 0.0001$) and 20% for *Quercus* (r = 0.567, $p < 0.0001$), using spline adjustment values (Fig.7C). Interestingly, the iWUE of *Quercus* was always greater (around 30% on average) than the iWUE of *Fagus*. Moreover, trends do not seem to have been linear over time: although the data is quite scattered, an acceleration of the iWUE increase occurs around the 1950s for *Fagus* and *Quercus*, and the iWUE of *Quercus* has reached a maximum (around 80 µmol mol^{-1}) after the 1980s, still higher than the iWUE of *Fagus*.

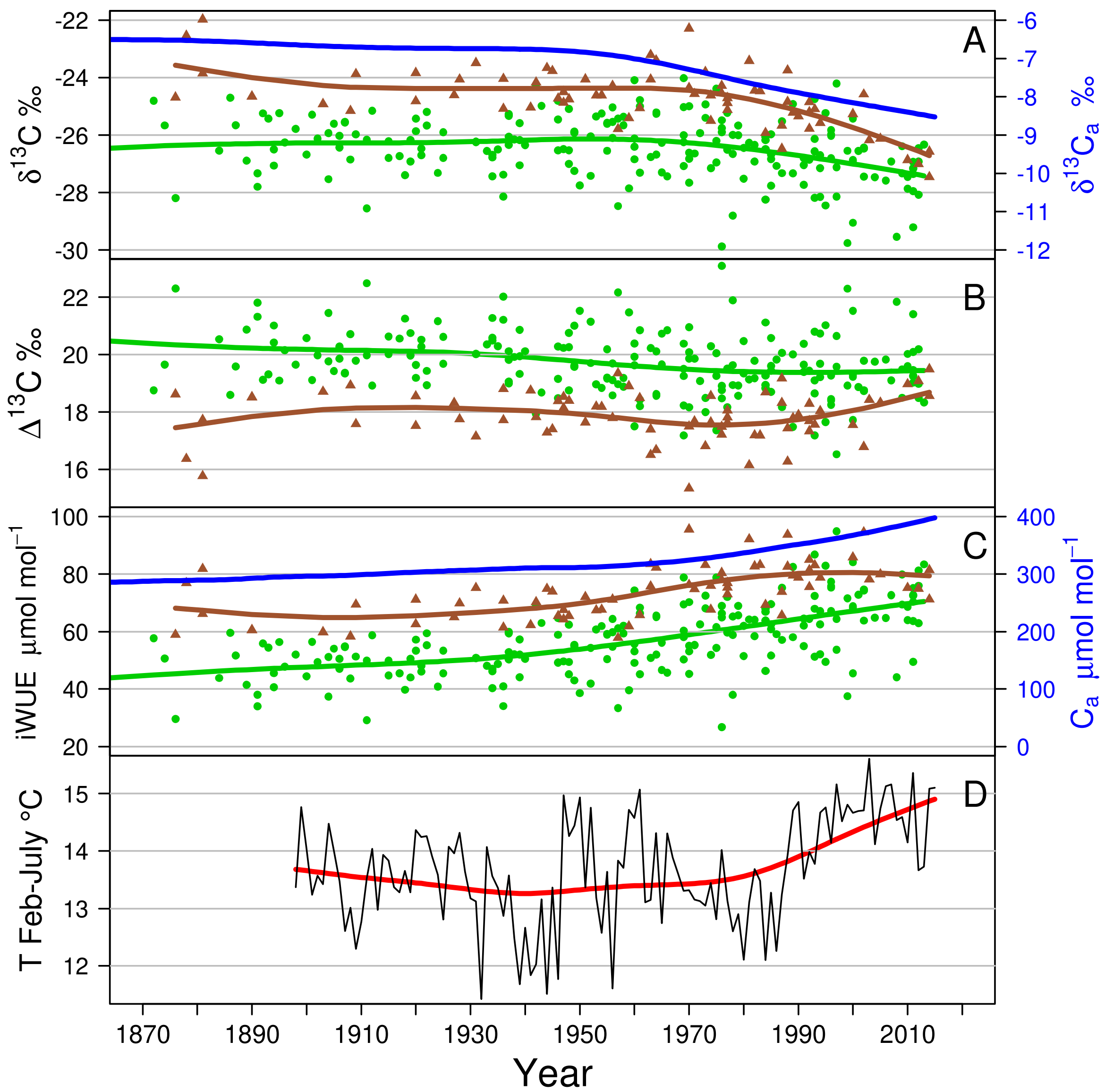

Figure 7. A. Mean δ^{13}C (‰) from tree rings of *Fagus* (green), *Quercus* (brown) and atmospheric CO_2 (in blue with right Y-axis) according to the year. B. Discrimination Δ^{13}C (‰). C. iWUE (µmol mol^{-1}) and atmospheric CO_2 concentration (in blue with right Y-axis). D. Mean temperature in February to July (black) fitted with a spline (red) at a climatic station located 20 km north of the forest under study.

For both species, iWUE increased with CO_2 concentration (C_a) at about the same rate until C_a reached about 345 µmol mol^{-1}, which corresponds to the CO_2 level in the mid 1980s (Fig.8). After that, *Fagus* iWUE continued to increase with C_a but at a lower pace, whereas *Quercus* iWUE stabilized at about 80 µmol mol^{-1}. In other words, the acceleration seen in Fig. 7 around the 1950s is mostly driven by a sharper increase in atmospheric CO_2 around the same period, while the 1980s seem to indicate a break point in the iWUE timeseries, where iWUE stops increasing as fast as CO_2, and even reaches a plateau in the case of *Quercus*.

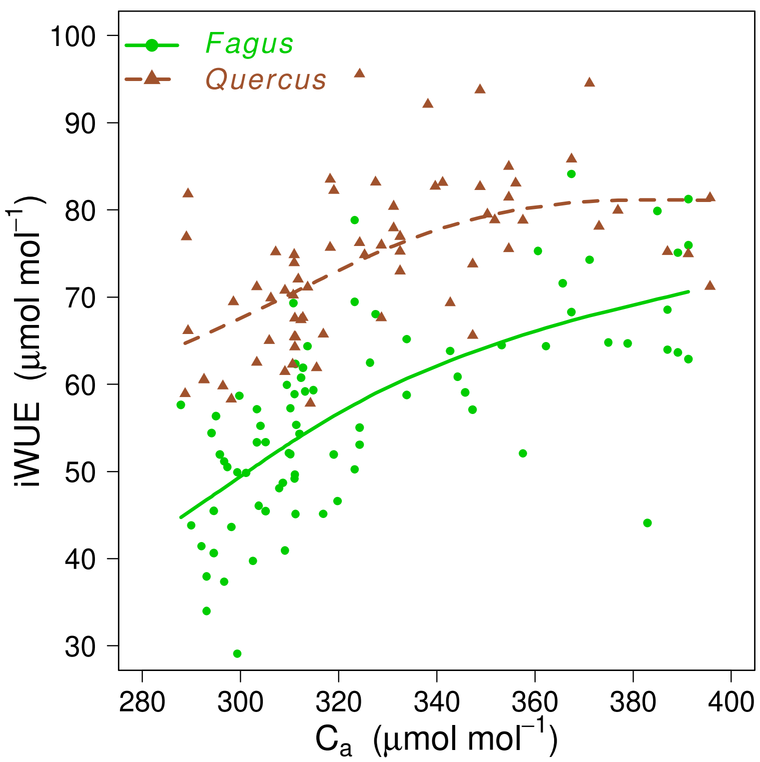

Figure 8. Intrinsic water-use efficiency (iWUE in µmol.mol^{-1}) in function of atmospheric CO_2 concentrations (C_a in µmol.mol^{-1}) for *Fagus* (green, n = 80) and *Quercus* (brown, n = 68), with spline fits. 290 µmol.mol^{-1} correspond to CO_2 concentrations during the 1870s.

4. DISCUSSION

8.1. Dynamics of growth and iWUE over the past 150 years

Standardization with the RCS method is robust and only retains long-term trends in the master chronologies (Esper et al., 2003; Bontemps et Esper, 2011). The comparison of the master chronologies (Fig.3) with the analysis of variance approach without standardization (Fig.4) led to almost the same trends but the temporal precision was higher with RCS. We conclude that, for both species, growth increased from *ca*. 1870 to 1920, then reached a plateau up to the mid 1950s with a sharp drop during the 1940s, then increased slightly up to the mid 1980s and finally decreased to reach the same level of the previous plateau (*Fagus*) or slightly below (*Quercus*).

The trends in iWUE derived from tree-ring $\delta^{13}C$ also bring some light on these growth patterns. But here again, it was important to check first that our sampling design did not influence the reported trends in iWUE. In our study, we found that cambial age had no significant influence on the isotopic composition of tree rings, with a constant mean value of around -26.5‰ (Fig.6). The lack of trend was tested here with the “slope of the mean”, and confirmed with the “mean of the slopes” method (McCarroll et al., 2020). This is in contrast with previous studies that showed variations in tree-ring $\delta^{13}C$ from pith to bark, albeit with different directions and amplitudes (Leavitt, 2010) depending on species, site or forest management (Duquesnay et al., 1998). Thus, some studies found that tree-ring $\delta^{13}C$ increased (Helama et al., 2015; Duquesnay et al., 1998), changed little (Bert et al., 1997) or decreased (Duquesnay et al., 1998) with cambial age. In beech high stand in north-eastern France, the most depleted tree-ring $\delta^{13}C$ values were attained before 50 yr-old (Duquesnay et al., 1998), which is indicative of a higher proportion of ^{13}C-depleted CO_2 respired by the soil and re-incorporated by young, small beech trees in the understorey. Differently, in the Ciron gorges, the linear structure of the forest limited to steep banks approximately oriented perpendicular to the dominant west winds may reduce air stratification and the accumulation of ^{13}C-depleted respired CO_2 in the understorey. Because of forest structure young and adult beech trees must experience similar isotopic composition of atmospheric CO_2 explaining why tree-ring $\delta^{13}C$ is almost constant from pith to bark, at least during the first 50 years. Consequently, the lack of age effect on tree-ring $\delta^{13}C$ allowed us to use all $\delta^{13}C$ measurements, regardless of cambial age, to study the evolution of iWUE over time.

Temporal trends in tree-ring $\delta^{13}C$-derived iWUE (Fig.7) can help explain some observed temporal changes in stem growth (Fig.3). Over the entire study period we identified two sub-periods in iWUE with a breakpoint in the mid 1980s common to the growth dynamics. Before 1980s, iWUE increased in parallel to the increase in atmospheric CO_2, but with higher values for *Quercus* than *Fagus*, while after the 1980s, the rate of increase of atmospheric CO_2 accelerated faster than that of iWUE, and the iWUE of *Quercus* even plateaued (Fig.7, 8). Over 1870-2015, iWUE increased by ca 50 % for *Fagus* and by 20 % for *Quercus*. This increase of iWUE with natural CO_2 enrichment of the studied populations agrees with elevated CO_2 (eCO_2) experiments in greenhouses. Heath and Kertiens (1997) showed that iWUE of *Fagus* seedlings was 114 % higher in eCO_2 (600 µmol mol^{-1}) and 84 % in *Quercus*. In this case, assimilation increased by +75 % in *Fagus*, while stomatal conductance decreased by -15 % (non-significant), compared to +33 % and -34 % in *Quercus*, respectively.

The plateauing of *Quercus* iWUE after the 1980s (Fig.8) is coherent with the conclusions from a meta-analysis on tree-ring $\delta^{13}C$-derived iWUE on mature trees growing in natural settings or in Free-air CO_2 enrichment (FACE) experiments (Voelker et al. 2016). This meta-analysis found that much of the CO_2-induced changes in iWUE (i.e. $\partial iWUE/\partial C_a$, a proxy for C_i/C_a, the ratio of CO_2 in the substomatal cavity C_i to the outside air C_a) occurred below 400 µmol mol^{-1} and that, at higher CO_2 levels, iWUE tended to level off because photosynthesis would reach a maximum and stomatal conductance a minimum. Larger CO_2-induced increase in photosynthetic rates may not be possible in natural settings because of other limiting factors to photosynthesis such as nutrient or water availability, and probably also light, as canopy closure is already attained in this riparian, unmanaged forest. This would be coherent with the maximum level of BAI observed before the 1980s in both species (Fig.4). Interspecific differences in iWUE are also very informative on the relationships between gas exchanges and growth. In 120-yr-old *F. sylvatica* and *Quercus petraea* stands, Jonard et al (2011) found differences in stomatal conductance that could be related to differences in sapwood-to-leaf area ratio: beech trees had a higher sapwood area than oaks and a stomatal conductance also about 1.8 times in conditions of good water supply. If we transpose these findings to the current study, and use the observed differences in BAI (about 1.2 greater for *Fagus* than for *Quercus* at 45-yr-old, see Fig.2) as a proxy for interspecific differences in photosynthetic rates, we conclude that the iWUE of *Fagus* should be about 0.7 times that of *Quercus*. In 1980, the mean $\delta^{13}C$-derived iWUE values were 60 µmol mol^{-1} for *Fagus* and 80 µmol mol^{-1} for *Quercus* (Fig.7C), which gives a ratio of 0.7, in good agreement with gas exchange estimates. Therefore, although environmental conditions differed between both studies, this back of the envelope calculation showed that the interspecific differences in iWUE and growth rates are coherent with differences in stomatal control with increasing CO_2 levels up to 1980s.

After the 1980s the average radial growth rate showed a slight (-6 % for *Fagus*) or stronger (-9.3 % for *Quercus*) lowering (Fig.3 and 4). During the same period, CO_2 levels increased more rapidly and the iWUE of *Fagus* continued to increase strongly while that of *Quercus* levelled off (Fig.7 and 8). The studied forest has not been submitted to major anthropogenic modifications since 1980 because its location in a valley with steep slopes keeps it excluded from silvicultural practices. To our knowledge, the main environmental factor which could have altered the growth capacity of the two species would be a fast warming of spring and summer (Fig.7D). However, it is difficult to demonstrate the mechanism of action of temperature, and several processes can be envisaged to understand these evolutions. It would be possible that a loss of carbohydrates occurs before wood biosynthesis. The higher respiration would cause a reduction in the amount of wood and a loss of carbon reserves at the end of the season, then a narrower initial wood of the following year. The respiration releases about 30-50 % of the fixed carbon, and increases exponentially with temperature (Damesin et al., 2002; Patterson et al., 2018). This may have already been the case during the studied 150 years, and thus partly reducing the growth increase during the period 1850-1980s. After 1980s, the hypothesis was that respiration could release a higher proportion of fixed carbon and reduce the amount of wood formed each year. This effect could be augmented by the effect of temperature on vapor pressure deficit through stomata mechanisms (Timofeeva et al., 2017) because both species close their stomata early when water supply decreases or atmospheric dryness increases (for *Fagus*, Aranda et al., 2015). Finally, whatever the reasons, it seems that temperature during growing season is becoming more important in recent years (Bosela et al., 2016; Mathias et Thomas, 2021).

9.1. From past to future: tree growth under climate drivers

The mean sensitivity is a dendrochronological parameter that indicates the strength of year-to-year variations. Its average value was 0.289 for *Fagus* (with many trees with MS=0.35 to 0.55) and 0.243 for *Quercus* (no tree with MS>0.35) (Table 1, Fig.S3 A&B), which is within the range of usual values in natural forests. In the Netherlands, a study of the effects of the 2003 drought showed that *Fagus* is able to recover faster than *Quercus* (Van der Werf et al., 2007). In the Ciron forest, the higher mean sensitivity for *Fagus* than for *Quercus* confirms that *Fagus* respond more strongly to climate and are able to recover faster after a stress. These sensitive growth series also revealed that the first-order correlation autocorrelation was generally positive and significant (Table 1, Fig.S3) which implies that climate of a given year modifies growth during two years and that it must be accounted for during growth modelling. The present work used proven methods in order to get parsimonious and easy-to-access climatic variables calibrated over 120 years. These models are site-specific because local conditions highlight different variables that express the predominant effect of a particular climatic factor (Latte et al., 2015; Sanchez-Salguero et al., 2017; Bert et al., 2020).

For *Fagus*, the most efficient model explained 42.4 % of the variance with only two climatic variables: the climatic water balance in June to September of the previous year and the climatic water balance from February to July of the current year. For *Quercus*, the best model explained 27.6 % of the variance with the mean temperature in previous October-November and the total precipitations in current April to August. These percentages of explained variance are of the same order as the values obtained in previous studies for both species (Lebourgeois et al., 2005; Mérian et al., 2011). Similarly, the most relevant variables were from the current year while the variables from the previous year were less correlated (Lebourgeois et al., 2005; Jump et al., 2007; Bauwe et al., 2015). However, this was not the case for temperature for *Quercus* because it was positively correlated with growth during previous autumn but not during the growing season. This is consistent with the dynamics of tree ring formation in *Quercus* because the earlywood forms in spring before the leaves open, with the energy of stored photosynthates which are in much greater quantity in *Quercus* than in *Fagus* (Barbaroux et Bréda, 2002; Richardson et al., 2013). Such a functioning is also in agreement with a lower mean sensitivity to climate in *Quercus* than in *Fagus* (Table1) because the buffering capacity is higher in *Quercus*.

The variables expressing water balance underline the importance of spring and summer weather conditions for *Fagus* growth in the Ciron valley, although this forest is located in an unusual proximity to a permanent river, but in a warmer climate than in the main part of the range. Differences in wood anatomy between the two species may also affect their resistance to water stress as vulnerability to embolism determines the limits of drought tolerance (Stojnic et al., 2018). Beech populations located in northern Europe are less resistant to embolism than those located in southern Europe, which experience higher water deficits. On the contrary, the Ciron population was one of the most vulnerable ones with a P50 of -3 MPa, either due to genetic variation or phenotypic plasticity

(Stojnic et al., 2018). Such forests showing low resistance to embolism would lose potential suitability based on average climate, which would lower their survival in the future under RCP4.5 climatic scenario (Stojnic et al., 2018). From purely climatic models, the projections for the future growth of *Fagus* and *Quercus* in the present study are not so pessimistic (Fig.5), especially with RCP4.5. It may be due to the Ciron site characteristics because the habitat suitability of this population was projected to be rather stable through time in the next decades under RCP4.5 scenario, whereas surrounding areas might lose habitat suitability (Stojnic et al., 2018). For *Quercus*, the P50 was -4,7 MPa in samples from sites near Bordeaux, i.e. an area outside the Ciron valley (Lobo et al., 2018). Therefore, *Quercus* is less vulnerable to embolism than *Fagus*, which is consistent with its lowest mean sensitivity to interannual variations of climate. On the contrary, such characteristics cannot explain the strongest decreasing trend after the 1980s in *Quercus* which seems to be due to others factors. When *Fagus* and *Quercus* are mixed on a deep soil, the soil layers are unevenly occupied by both species: the *Fagus* shallow rooting system is rather concentrated in the upper layers of the soil while the *Quercus* explores more the deep layers (Lebourgeois et Jabiol, 2002; Packham et al. 2012). However, the stony and superficial soils of the Ciron valley do not allow such a stratification (Barbeta et al., 2019) and *Fagus* outcompete *Quercus*. The stronger downward trend shown by *Quercus* since the 1980s would be consistent with this behaviour.

On the entire time period considered in the present study, the climatic models fitted rather well the past interannual and long-term trends of growth (Fig.5). For the future, the predictions of growth were surprisingly close to each other with both RCMs and RCP pathways. For *Fagus*, the trend would be a not significant slight decrease of growth, excepted in the case of RCP 8.5 with Aladin RCM climatic data predictions which would predict a strong and significant loss of growth level. For *Quercus*, the four cases would be similar and predict a very slight not significant increase, which would be higher under RCP 4.5 scenario (significant with Aladin RCM). Similarly to the present study, Bauwe et al (2015) modelled tree growth with different time scales of climatic variables and injected predicted climatic conditions until 2100 in their model to predict future growth for forest species in Germany. They showed that the growth index of common beech and pedunculate oak will likely decrease between 8 to 23 % according to species and region of Germany, under A1B scenario (IPCC 2007) which is intermediate between RCP 4.5 and RCP 8.5. Differently, in the Ciron valley, *Fagus* growth index would decrease by only 5 to 13 % with not significant slopes (Fig.5), except in the case of the most warming scenario and model combination (RCP 8.5 with Aladin RCM) which would significantly decrease growth by 50 %.

Quercus growth index would change very little with only one significant increase by circa 15 % in the case of RCP 4.5 and Aladin RCM. Therefore, it seems that the environment of the refuge of the Ciron Valley can buffer the effects of long-term changes on the answer of trees to mean climate, even if this site is at the west-edge for beech distribution. The previous assumptions, although quite reassuring, may still be too pessimistic since our study could not consider the evolution of phenology. The spring temperature determines the start and the autumn temperature determines the end of cambial activity. The future climate could therefore lengthen the wood formation period and thus lead to an increase in growth (Prislan et al., 2019). For the Ciron region, predictions indicate a significant increase in temperature in September-October (RCP4.5) or throughout the year (RCP8.5, data not shown), which could lead to a longer growth period. Furthermore, our predictions were projected to 2100, whereas previous studies went to 2050 (Stojnic et al., 2018) or 2080 (Prislan et al., 2019). This may explain the significant decreasing trend in growth for *Fagus* as the predicted values are significantly lower after 2070 (Fig.5).

The location of this population in a valley far from the main part of the natural range of beech precludes migration to the north when climate warms. The only survival solution for the species is to endure the new conditions, which seems possible according to our results for the whole population. Moreover, some parts of the valley could help to better withstand global warming. Temperature measurements outside the valley and at different positions in the valley showed that the bottom of the valley is 2-3°C cooler than the top in summer (Walbott, 2018). Among the stand, the competition between species (beech vs oak) would also regulate the level of growth of each species (Pretzsch et al., 2013). A study in southern Germany on *Fagus sylvatica* and *Quercus petraea* demonstrated that beech in mixed stands with oak showed less reduction in growth during a drought in a mixed stand than in a pure beech forest, whereas the oak did not benefit from this mixed effect (Pretzsch et al., 2013). Such interactions in mixed stands with beech were also found to depend on species identity in southern Alps during the 4-5 years after a drought stress (Jourdan et al., 2019).

10.1. Focus on range-edge vs range-core populations

Tree-ring $\delta^{13}C$ values in this study are between -27 and -25‰. This is more depleted than those of north-eastern French beech populations, around -25 and -23‰ (Duquesnay et al., 1998). Tree-ring $\delta^{13}C$ values in the Ciron valley (at an altitude of 30-50 m) were closer to values found at higher altitudes

(1200-1600 m) in the Spanish Pyrenees with mean annual precipitation of *ca*. 1000 mm (Peñuelas et al., 2008). Since tree-ring $\delta^{13}C$ values are generally higher when conditions are drier, this discrepancy in average values is indicative of wetter conditions in the Ciron valley compared to north-eastern France, possibly through precipitation regimes (average annual rainfall 812 mm vs 730 mm in northeast France) or other environmental factors not characterized in the present study.

The sample covered a range from 32 to 205 years old for *Fagus* and 47 to 245 years old for *Quercus*. The maximum natural age of *Fagus* of about 200 years suggests that this population is not at its ecological optimum, as significantly older beeches can be found in the mountains, e.g. up to 478 years in the Pyrenees Mountains 200 km south of Ciron valley (Bourquin-Mignot & Girardclos, 2001). In the Ciron valley, *Fagus* has a maximum growth rate of 27 cm^2/year, which is similar in northeast France in lowland (Badeau et al., 1995) or mountains (Picard, 1995). However, the maximum is reached at around 80 years in the Ciron valley whereas it takes 120 years in northeast France, and the following decline is faster in the Ciron valley. For *Quercus*, BAI peaks at 19 cm^2/year at 50 years-old in the Ciron valley, then decreases very slowly. The dynamics is different in the northeast of France (Becker et al., 1994) where BAI slowly increases until the age of 150 years old and reaches 17 cm^2/year, passing by the value of only 8 cm^2/year at 50 years-old. Finally, it seems that the growth dynamics in the Ciron valley is a temporal concentration of what can happen further inside the range-core: growth increases rapidly and also decreases rapidly with ageing, which is consistent with a shorter longevity.

The long-term growth trends shown by both studied species in the Ciron valley seem to be only partly in agreement with other locations. *Fagus* showed increasing trends over 1880-1990 in the lowlands and the Vosges mountains of north-eastern France (Badeau et al., 1996), and *Quercus* also showed an increasing trend over 1890-1987 (Becker et al., 1994). However, these early studies could not show what happened after the 1980s. Later on, the previous increasing trends have been confirmed and decreasing trends since the 1980s were documented: -18 % in even-aged stands in north-eastern France (Bontemps and Esper, 2011), -49 % in the Spanish Pyrenees at low altitude (Jump et al., 2006), -25 % in the Central Apennines in Italy between 1970s and 2000s (Piovesan et al., 2005). With the methods of forest surveys over 1970s-2000s (Charru et al., 2017), beech showed a maximum growth in the 1990s and started a slight decreasing trend afterwards while the pedunculate oak showed a stable growth over time. Likewise, the growth of *Fagus* and *Quercus* in southern Germany showed no trend towards reduced growth after the 1980s (Pretzsch et al., 2013). Further east, in Slovakia, beech growth increased between 1960s and 1990s, then it slowed down or decreased depending on thinning intensity (Bosela et al., 2016). The intensity of these trends therefore differs between studies, in particular because they depend on the fertility of the forest site and the age vs year balanced sampling (Becker at al., 1995; Bontemps et Esper, 2011). The response to climate is also often involved in these slow evolutions over time. In our study, the most likely predictions for tree growth up to the end of the 21st century have been obtained with parsimonious statistical climatic models established over past periods. The predicted trends are weaker than in other situations, suggesting that this site has some sort of buffering power against climate change. These predictions will be valid if the principle of uniformity is applied over time (Wilmking et al., 2020), and if pathogens, management, or functional relationships remain stable.

Studies on a global scale and in Europe have shown that trees are able to increase their water-use efficiency as atmospheric CO_2 concentrations levels rise (Waterhouse et al., 2004; Peñuelas et al., 2011; Tognetti et al., 2014; Frank et al., 2015). Such an increase in the iWUE is often accompanied by an increase of plant growth due to the high atmospheric CO_2 concentration effect on A and the reduced water consumption of plants (González de Andrés et al. 2018). However, an increase in iWUE does not necessarily translates into an increase in beech growth for low-altitude populations at the southern range edge of this species in Europe (Peñuelas et al., 2008). Then, models based on many biological processes could better assess the consequences of climate conditions (Kramer et al., 2010). Indeed, this type of approach has already showed evolutions quite comparable to our results concerning the evolution of iWUE during the last century. For example, the process-based model "LPX-Bern" was in good agreement with tree-rings records from north hemisphere which suggested on average an increase of +27 % of iWUE since 1900 (Keller et al., 2017). This order of magnitude is similar to circa +30 % found for *Fagus* in north-east France between 1880s and 1990s with tree-ring $\delta^{13}C$ analysis (Duquesnay et al., 1998), and similar to +33 % for *Fagus* and +18 % for *Quercus* since 1900 in the Ciron site. This suggests that the local environmental conditions of this refuge offer the possibility to behave as in some regions of the main range although the regional climate of southwestern France is less favourable for common beech. Ecosystems are not uniformly affected by climate warming and some species will be more resilient than others due to local site conditions, in particular among the regions of the southern limit of distribution (Vilà-Cabrera et Jump, 2019).

5. CONCLUSION

The studied beech forest is the remaining part of a larger pre-glacial stand which has lasted for at least 30,000 years in the small canyon of the Ciron river in southwestern France (De Lafontaine et al., 2014). This stand also includes oak and other deciduous species in smaller quantities. In this range-edge site, the beeches and pedunculate oaks reach a maximum age of 250 years and their growth is in the same order of magnitude than in range-core area. Radial growth of both species increased during 1870s to 1980s, then slightly decreased during 1980s to 2010s, in agreement with some other beech and oak forests in western Europe. During the same period of time, iWUE of beech also increased continuously while iWUE of oak levelled off since the 1980s, when the decreasing trend of growth was stronger for oak. Modelling showed that climatic water balance was the prevailing factor for beech growth, although this stand borders a permanent river. When the climate predictions from the RCP scenarios are fed into the models obtained for this site, the growth predictions for 2020s-2100s showed mainly non-significant trends for beech and oak, with significant decreasing trend for beech and significant increasing trend for oak in climatic scenarios RCP4.5 or RCP8.5 transcribed locally by the Regional Climatic Model Aladin. In summary, the future growth will probably not change to a large extend with the hypothesis that the parsimonious linear models built in the present study will remain valid under global change.

The long-term increasing trends are consistent with a slow evolution of iWUE if the carbon assimilation increased under air CO_2 enrichment accompanied by a possible reduction of the stomatal conductance for water (Mathias and Thomas, 2021). The soil-atmosphere hydraulic chain is composed of various steps which can modify species responses to drought and temperature. The process may differ according to the considered time scale from annual (climatic stress during one growing season), decadal (several stress during following years) to long term (a slow evolution of average characteristics of the climate or the CO_2 rate). The refuge effects in the Ciron valley could change partly some of these processes compared to core-range and modify the potential of beech to acclimate to diverse environmental conditions. This site is located at geographical marginality but growth and functioning patterns showed that this ecosystem is less in ecological marginality, which increases its persistence probability. Complementarity effects between tree species should be also considered because beech copes better with drought stress when mixed with oak, especially since the 1980s when temperature increased significantly. A diversified forest, with different species and a staggering of trees in the understorey, would give better resistance to drought and warming stress (Pretzsch et al., 2013; Bosela et al., 2016). These traits will help some beech forests to survive outside the main range, like they did in the past. However, the small size of the beech population requires human protection to ensure its long-term survival. For example, work is underway to increase the number of young beech trees from this population, and to protect this original genetic resource in plantations located in the range-core area (Ouayjan et Hampe, 2018).

ACKNOWLEDGEMENTS

We thank P. Reynet (who remains in our memories), R. Ségura, G. Gerzabek, X. Capdevielle, and C. Lambrot for the help with field sampling and laboratory measurements. A. Quenu, S. Irola and M. Laprie provided valuable support with sampling permits and logistics. The authors would like to thank SILVATECH (Structural and functional analysis of tree and wood Facility, doi: 10.15454/1.5572400113627854E12) for its contribution to isotopic analysis. Meteo-France climatic data were extracted from the INRA CLIMATIK database. The study received financial support from the Agence de l'Eau Adour-Garonne (contract INRA 22000961 AEAG 310 33 0128), the Conseil Régional d'Aquitaine (project RELICT 2014-1R20603), and the French National Research Agency (ANR) in the frame of the Investments for the future Program, within the Cluster of Excellence COTE (ANR-10-LABX-45, project CLIMBEECH). The topographic map in Fig1 is from geoportail.gouv.fr edited by Institut National de l'Information Géographique et Forestière, Paris (ISSN 2490-9068).

DATA AVAILIBILITY

The datasets generated and analysed during the current study will be available in the DATAINRA repository.

REFERENCES

Allen, C.D., Macalady, A.K., Chenchouni, H., Bachelet, D., McDowell, N., Vennetier, M., Kitzberger, T., Rigling, A., Breshears, D.D., Hogg, E.H. (Ted), Gonzalez, P., Fensham, R., Zhang, Z., Castro, J., Demidova, N., Lim, J.-H., Allard, G., Running, S.W., Semerci, A., Cobb, N., 2010. A global overview of drought and heatinduced tree mortality reveals emerging climate change risks for forests. Forest Ecology and Management 259, 660–684. DOI: 10.1016/j.foreco.2009.09.001

Aranda, I., Cano, F.J., Gascó, A., Cochard, H., Nardini, A., Mancha, J.A., López, R., Sánchez-Gómez, D., 2015. Variation in photosynthetic performance and hydraulic architecture across European beech (*Fagus sylvatica* L.) populations supports the case for local adaptation to water stress. Tree Physiology 35:1, 34-46. DOI: 10.1093/treephys/tpu101

Bachtobji Bouachir, B., Khorchani, A., Guibal, F., El Aouni, M., & Khaldi, A., 2017. Dendroecological study of *Pinus halepensis* and *Pinus pinea* in northeast coastal dunes in Tunisia according to distance from the shoreline and dieback intensity. Dendrochronologia 45, 62-72. DOI: 10.1016/j.dendro.2017.06.008

Badeau V., Dupouey J.-L., Becker M., Picard J.-F., 1995. Long-term growth trends of *Fagus sylvatica* L in northeastern France. A comparison between high and low density stands. Acta Oecologica 16:5, 571-583. hal-02701943

Badeau, V., Becker, M., Bert, D., Dupouey, J.-L., Lebourgeois, F., Picard, J.-F., 1996. Long-term growth trends of trees: ten years of dendrochronological studies in France. In: Spiecker, H., Mielikäinen, K., Köhl, M., Skovsgaard, J.P. (Eds.), Growth Trends in European Forests. Springer Berlin Heidelberg, Berlin, Heidelberg. European Forest Institute Research Report 5, 167-181

Barbaroux, C., Bréda, N., 2002. Contrasting distribution and seasonal dynamics of carbohydrate reserves in stem wood of adult ring-porous sessile oak and diffuse-porous beech trees. Tree Physiology 22: 1201–1210. DOI: 10.1093/treephys/22.17.1201

Barbeta, A., Jones, S.P., Clavé, L., Wingate, L., Gimeno, T.E., Fréjaville, B., Wohl, S., Ogée, J. 2019. Unexplained hydrogen isotope offsets complicate the identification and quantification of tree water sources in a riparian forest. Hydrology and Earth System Sciences 23: 2129–2146. DOI: 10.5194/hess-23-2129-2019

Bauwe, A., Jurasinski, G., Scharnweber, T., Schröder, C., Lennartz, B., 2015. Impact of climate change on tree-ring growth of Scots pine, Common beech and Pedunculate oak in northeastern Germany. iForest e1-e11. DOI: 10.3832/ifor1421-008

Becker, M., 1989. The role of climate on present and past vitality of silver fir forests in the Vosges mountains of northeastern France. Canadian Journal of Forest Research 19, 1110–1117. DOI: 10.1139/x89-168

Becker, M., Bert, D., Bouchon, J., Dupouey, J.-L., Picard, J.-F., Ulrich, E. 1995. Long-term changes in forest productivity in northeastern France: the dendroecological approach. In: Landmann, G., Bonneau, M., Kaennel, M. (eds). Forest decline and atmospheric deposition effects in the French mountains. DOI: 10.1007/978-3-642-79535-0_5

Becker, M., Nieminen, T.M., Gérémia, F., 1994. Short-term variations and long-term changes in productivity in northeastern France. The role of climate and atmospheric CO_2. Annales des Sciences Forestières 51:5, 477–492. DOI : 10.1051/forest:19940504

Bert, D., 1993. Impact of ecological factors, climatic stresses and pollution on growth and health of silver fir (*Abies alba* Mill.) in the Jura mountains: an ecological and dendrochronological study. Acta Oecologica 14, 2, 229-246

Bert, D., Leavitt, S.W., Dupouey, J.-L., 1997. Variations of wood $\delta^{13}C$ and water-use efficiency of *Abies alba* during the last century. Ecology 78, 1588–1596. DOI: 10.1890/0012-9658(1997)078[1588:VOWCAW]2.0.CO;2

Bert, D., Lebourgeois, F., Ponton, S., Musch, B., Ducousso, A., 2020. Which oak provenances for the 22nd century in Western Europe? Dendroclimatology in common gardens. PLoS ONE 15(6): e0234583. DOI: 10.1371/journal.pone.0234583

Bontemps, J., Esper, J., 2011. Statistical modelling and RCS detrending methods provide similar estimates of long-term trend in radial growth of common beech in north-eastern France. Dendrochronologia 29:2, 99-107. DOI: 10.1016/j.dendro.2010.09.002

Bosela, M., Štefančík, I., Petráš, R., Vacek, S., 2016. The effects of climate warming on the growth of European beech forests depend critically on thinning strategy and site productivity. Agricultural and Forest Meteorology 222, 21-31. DOI: 10.1016/j.agrformet.2016.03.005

Bourquin-Mignot C., Girardclos O., 2001. Construction d'une longue chronologie de hêtres au Pays-Basque. La forêt d'Iraty et le Petit Age Glaciaire. Sud-Ouest Européen 11, 59-71. https://www.persee.fr/doc/rgpso_1276-4930_2001_num_11_1_2767

Briffa, K., Melvin, T.M., 2011. A closer look at regional curve standardization of tree-ring records: Justification of the need, a warningof some pitfalls, and suggested improvements in its application. Dendroclimatology: Progress and Prospects, edited by Hughes, M.K. et al., Springer, Dordrecht, Netherlands, pp. 113–146. DOI: 10.1007/978-1-4020-5725-0_5

Bruhn, D., Leverenz, J., Saxe, H., 2000. Effects of tree size and temperature on relative growth rate and its components of *Fagus sylvatica* seedlings exposed to two partial pressures of atmospheric [CO2]. New Phytologist 146:3, 415-425. DOI: 10.1046/j.1469-8137.2000.00661.x

Bunn, A.G., 2008. A dendrochronology program library in R (dplR). Dendrochronologia 26, 115–124. DOI: 10.1016/j.dendro.2008.01.002

Cailleret, M., Jansen, S., Robert, E.R., DeSoto, L., Aakala, T., Antos, J.A., et al., 2016. A synthesis of radial growth patterns preceding tree mortality. Global Change Biology 23:4, 1675-1690. DOI: 10.1111/gcb.13535

Cavin, L., Jump, A.S., 2016. Highest drought sensitivity and lowest resistance to growth suppression are found in the range core of the tree *Fagus sylvatica* L. not the equatorial range edge. Global Change Biology 23, 362–379. DOI: 10.1111/gcb.13366

Chambers, J.M., Hastie, T.J., 1992. Statistical models in S. Wadsworth and Brooks/Cole. 608 p.

Charru, M., Seynave, I., Hervé, J.-C., Bertrand, R., Bontemps, J.-D., 2017. Recent growth changes in Western European forests are driven by climate warming and structured across tree species climatic habitats. Annals of Forest Science 74, 1-34. DOI: 10.1007/s13595-017-0626-1

Cheaib, A., Badeau, V., Boe, J., Chuine, I., Delire, C., Dufrêne, E., François, C., Gritti, E.S., Legay, M., Pagé, C., Thuiller, W., Viovy, N., Leadley, P., 2012. Climate change impacts on tree ranges: model intercomparison facilitates understanding and quantification of uncertainty: Understanding and quantification of uncertainties of climate change impacts on tree range. Ecology Letters 15, 533–544. DOI: 10.1111/j.1461-0248.2012.01764.x

Cook, E.R., Kairiukstis, L.A., 1990. Methods of Dendrochronology: Applications in the Environmental Sciences. Springer. ISBN-13: 978-0-7923-0586-6

Cook, E.R., Peters, K., 1981. The smoothing spline: a new approach to standardizing forest interior tree-ring width series for dendroclimatic studies. Tree-Ring Research 41, 45-53. ISSN 0041-2198

Craig, H., 1957. Isotopic standards for carbon and oxygen and correction factors for mass-spectrometric analysis of carbon dioxide. Geochimica et Cosmochimica Acta 12, 133–149

Damesin, C., Ceschia, E., Le Goff, N., Ottorini, J.-M., Dufrêne, E. 2002. Stem and branch respiration of beech: from tree measurements to estimations at the stand level. New Phytologist 153:1, 159-172. DOI: 10.1046/j.0028-646X.2001.00296.x

Damesin, C., Lelarge, C., 2003. Carbon isotope composition of current-year shoots from *Fagus sylvatica* in relation to growth, respiration and use of reserves. Plant, Cell and Environment 26, 207-219.DOI: 10.1046/j.1365-3040.2003.00951.x

Dawson, T.E., Mambelli, S., Plamboeck, A.H., Templer, P.H., Tu, K.P., 2002. Stable Isotopes in Plant Ecology. Annual Review of Ecology and Systematics 33, 507–559. DOI: 10.1146/annurev.ecolsys.33.020602.095451

De Lafontaine, G., Amasifuen Guerra, C.A., Ducousso, A., Petit, R.J., 2014. Cryptic no more: soil macrofossils uncover Pleistocene forest microrefugia within a periglacial desert. New Phytologist 204, 715–729. DOI: doi.org/10.1111/nph.12833

De Lafontaine, G., Ducousso, A., Lefèvre, S., Magnanou, E., Petit, R. J., 2013. Stronger spatial genetic structure in recolonized areas than in refugia in the E uropean beech. Molecular Ecology 22 :17, 4397-4412. DOI : 10.1111/mec.12403

Dobrowski, S.Z., 2011. A climatic basis for microrefugia: the influence of terrain on climate. Global Change Biology 17, 1022–1035. DOI: 10.1111/j.1365-2486.2010.02263.x

Dorado-Liñán, I., Piovesan, G., Martínez-Sancho, E., Gea-Izquierdo, G., Zang, C., Cañellas, I., Castagneri, D., Di Filippo, A., Gutiérrez, E., Ewald, J., Fernández-de-Uña, L., 2019. Geographical adaptation prevails over species-specific determinism in trees' vulnerability to climate change at Mediterranean rear-edge forests. Global Change Biology 25, 1296-1314. DOI: 10.1111/gcb.14544

Duquesnay, A., Bréda, N., Stievenard, M., Dupouey, J.-L., 1998. Changes of tree-ring $\delta^{13}C$ and water-use efficiency of beech (*Fagus sylvatica* L.) in north-eastern France during the past century. Plant, Cell and Environment 21, 565–572. DOI: 10.1046/j.1365-3040.1998.00304.x

Ehleringer, J., Hall, A., Farquhar, G., 1993. Stable isotopes and plant carbon–water relations. Agricultural and Forest Meteorology 72, 555 pp. ISBN 0-12-233380-2

Ehleringer, J.R., Rundel, P.W., 1989. Stable Isotopes: History, Units, and Instrumentation. In: Rundel P.W., Ehleringer J.R., Nagy K.A. (eds). Stable Isotopes in Ecological Research. Ecological Studies (Analysis and Synthesis) 68. Springer, New York, NY. DOI: 10.1007/978-1-4612-3498-2_1

Esper, J., Cook, E.R., Krusic, P.J., Peters, K., Schweingruber, F.H., 2003. Tests of the RCS method for preserving low-frequency variability in long tree-ring chronologies. Tree-Ring Research 59, 81–98.

Farquhar, G., O'Leary, M., Berry, J., 1982. On the relationship between carbon isotope discrimination and the intercellular carbon dioxide concentration in leaves. Functional Plant Biology 9, 121–137. DOI: 10.1071/PP9820121

Farquhar, G., Richards, R., 1984. Isotopic composition of plant carbon correlates with water-use efficiency of wheat genotypes. Functional Plant Biology 11, 539–552. DOI: 10.1071/PP9840539

Farquhar, G.D., Ehleringer, J.R., Hubick, K.T., 1989. Carbon isotope discrimination and photosynthesis. Annual Review of Plant Physiology and Plant Molecular Biology 40, 503-537.

Frank, D.C., Poulter, B., Saurer, M., Esper, J., Huntingford, C., Helle, G., Treydte, K., Zimmermann, N.E., Schleser, G.H., Ahlström, A., Ciais, P., Friedlingstein, P., Levis, S., Lomas, M., Sitch, S., Viovy, N., Andreu-Hayles, L., Bednarz, Z., Berninger, F., Boettger, T., D'Alessandro, C.M., Daux, V., Filot, M., Grabner, M., Gutierrez, E., Haupt, M., Hilasvuori, E., Jungner, H., Kalela-Brundin, M., Krapiec, M., Leuenberger, M., Loader, N.J., Marah, H., Masson-Delmotte, V., Pazdur, A., Pawelczyk, S., Pierre, M., Planells, O., Pukiene, R., Reynolds-Henne, C.E., Rinne, K.T., Saracino, A., Sonninen, E., Stievenard, M., Switsur, V.R., Szczepanek, M., Szychowska-Krapiec, E., Todaro, L., Waterhouse, J.S., Weigl, M., 2015. Water-use efficiency and transpiration across European forests during the Anthropocene. Nature Climate Change 5, 579–583. DOI: 10.1038/nclimate2614

Fritts H.C., 2012. Tree rings and climate. Elsevier. ISBN 0323145280, 9780323145282. 582 pp

García-Suárez, A., Butler, C., Baillie, M., 2009. Climate signal in tree-ring chronologies in a temperate climate: A multi-species approach. Dendrochronologia 27:3, 183-198. DOI: 10.1016/j.dendro.2009.05.003

Geßler, A., Keitel, C., Kreuzwieser, J., Matyssek, R., Seiler, W., Rennenberg, H., 2007. Potential risks for European beech (*Fagus sylvatica* L.) in a changing climate. Trees 21, 1–11. DOI: 10.1007/s00468-006-0107-x

Gillner, S., Rüger, N., Roloff, A., Berger, U., 2013. Low relative growth rates predict future mortality of common beech (*Fagus sylvatica* L.). Forest Ecology and Management 302, 372–378. DOI: 10.1016/j.foreco.2013.03.032

González de Andrés, E., Camarero, J.J., Blanco, J.A., Imbert, J.B., Lo, Y.-H., Sangüesa-Barreda, G., Castillo, F.J., 2018. Tree-to-tree competition in mixed European beech-Scots pine forests has different impacts on growth and water-use efficiency depending on site conditions. Journal of Ecology 106, 59–75. DOI: 10.1111/1365-2745.12813

Hampe, A., Jump, A.S., 2011. Climate Relicts: Past, Present, Future. Annual Review of Ecology, Evolution, and Systematics 42, 313–333. DOI: 10.1146/annurev-ecolsys-102710-145015

Hampe, A., Petit, R.J., 2005. Conserving biodiversity under climate change: the rear edge matters: Rear edges and climate change. Ecology Letters 8, 461–467. DOI: 10.1111/j.1461-0248.2005.00739.x

Heath, J., Kerstiens, G., 1997. Effects of elevated CO_2 on leaf gaz exchange in beech and oak at two levels of nutrient supply:consequences for sensitivity to droughtin beech. Plant, Cell and Environment 20: 57-67. DOI: 10.1046/j.1365-3040.1997.d01-13.x

Helama, S., Arppe, L., Timonen, M., Mielikänen, K., Oinonen, M., 2015. Age-related trends in subfossil tree-ring $\delta^{13}C$ data. Chemical Geology 416, 28-35. DOI: 10.1016/j.chemgeo.2015.10.019

Herrick, J.D., Maherali, H., Thomas, R.B., 2004. Reduced stomatal conductance in sweetgum (*Liquidambar styraciflua*) sustained over long-term CO_2 enrichment. New Phytologist 162, 387-396. DOI: 10.1111/j.1469-8137.2004.01045.x

Hughes, L., 2000. Biological consequences of global warming: is the signal already apparent? Trends in Ecology & Evolution 15, 56–61. DOI: 10.1016/S0169-5347(99)01764-4

IPCC. Climate Change 2014: Synthesis Report. Contribution of Working Groups I, II and III to the Fifth Assessment Report of the Intergovernmental Panel on Climate Change [Core Writing Team, R.K. Pachauri and L.A. Meyer (eds.)]. 2014; Geneva, Switzerland. ISBN: 978-92-9169-143-2

Jonard, F., André, F., Ponette, Q., Vincke, C., Jonard, M., 2011. Sap flux density and stomatal conductance of European beech and common oak trees in pure and mixed stands during the summer drought of 2003. Journal of Hydrology 409:1-2, 371-381. DOI: 10.1016/j.jhydrol.2011.08.032

Jourdan, M., Lebourgeois, F., Morin, X., 2019. The effect of tree diversity on the resistance and recovery of forest stands in the French Alps may depend on species differences in hydraulic features. Forest Ecology and Management 450, 117486. DOI: 10.1016/j. foreco.2019.117486

Jump, A. S., Ruiz-Benito, P., Greenwood, S., Allen, C. D., Kitzberger, T., Fensham, R., Martínez-Vilalta, J., Lloretet, F., 2017. Structural overshoot of tree growth with climate variability and the global spectrum of drought-induced forest dieback. Global Change Biology 23, 3742–3757. DOI: 10.1111/gcb.13636

Jump, A.S., Hunt, J.M., Peñuelas, J., 2006. Rapid climate change-related growth decline at the southern range edge of *Fagus sylvatica*. Global Change Biology 12, 2163–2174. DOI: 10.1111/j.1365-2486.2006.01250.x

Jump, A.S., Hunt, J.M., Peñuelas, J., 2007. Climate relationships of growth and establishment across the altitudinal range of *Fagus sylvatica* in the Montseny Mountains, northeast Spain. Ecoscience 14, 507–518. DOI: 10.2980/1195-6860(2007)14[507:CROGAE]2.0.CO;2

Jump, A.S., Mátyás, C., Peñuelas, J., 2009. The altitude-for-latitude disparity in the range retractions of woody species. Trends in Ecology & Evolution 24, 694–701. DOI: 10.1016/j.tree.2009.06.007

Keenan, T.F., Hollinger, D.Y., Bohrer, G., Dragoni, D., Munger, J.W., Schmid, H.P., Richardson, A.D., 2013. Increase in forest water-use efficiency as atmospheric carbon dioxide concentrations rise. Nature 499, 324–327. DOI: 10.1038/nature12291

Keller, K.M., Lienert, S., Bozbiyik, A., Stocker, T.F., Churakova (Sidorova), O.V., Frank, D.C., Klesse, S., Koven, C.D., Leuenberger, M., Riley, W.J., Saurer, M., Siegwolf, R., Weigt, R.B., Joos, F., 2017. 20^{th} century changes in carbon isotopes and water-use efficiency: tree-ring-based evaluation of the CLM4.5 and LPX-Bern models. Biogeosciences 14, 2641–2673. DOI: 10.5194/bg-14-2641-2017

Kramer, K., Degen, B., Buschbom, J., Hickler, T., Thuiller, W., Sykes, M.T., de Winter, W., 2010. Modelling exploration of the future of European beech (*Fagus sylvatica* L.) under climate change—Range, abundance, genetic diversity and adaptive response. Forest Ecology and Management 259, 2213–2222. DOI: doi.org/10.1016/j.foreco.2009.12.023

Latte, N., Lebourgeois, F., Claessens, H., 2015. Increased tree-growth synchronization of beech (*Fagus sylvatica* L.) in response to climate change in northwestern Europe. Dendrochronologia 33, 69-77. DOI: 10.1016/j.dendro.2015.01.002

Leavitt, S., 2010. Tree-ring C–H–O isotope variability and sampling. The Science of the Total Environment 408:22, 5244-5253. DOI:10.1016/j.scitotenv.2010.07.057

Leavitt, S.W., Danzer, S.R., 1993. Method for batch processing small wood samples to holocellulose for stable-carbon isotope analysis. Analytical Chemistry 65, 87-89.

Leavitt, S.W., Long, A., 1989. Drought indicated in $^{13}C/^{12}C$ ratios of south western tree rings. Water Resource Bulletin 25:341–47. DOI: 10.1111/j.1752-1688.1989.tb03070.x

Lebourgeois, F., Bréda, N., Ulrich, E., Granier, A., 2005. Climate-tree-growth relationships of European beech (*Fagus sylvatica* L.) in the French Permanent Plot Network (RENECOFOR). Trees 19, 385–401. DOI: 10.1007/s00468-004-0397-9

Lebourgeois, F., Jabiol, B., 2002. Enracinements comparés du Chêne sessile, du Chêne pédonculé et du Hêtre. (A comparison of the soil-root complex of Sessile oak, Pedunculate oak and Common beech). Revue Forestière Française 54:1, 17-42. DOI: 10.4267/2042/4898

Lebourgeois, F., Piedallu, C., 2005. Appréhender le niveau de sécheresse dans le cadre des études stationnelles et de la gestion forestière à partir d'indices bioclimatiques. Revue Forestière Française 57:3, 331-356. DOI: 10.4267/2042/5055

Lindner, M., Maroschek, M., Netherer, S., Kremer, A., Barbati, A., Garcia-Gonzalo, J., Seidl, R., Delzon, S., Corona, P., Kolström, M., Lexer, M.J., Marchetti, M., 2010. Climate change impacts, adaptive capacity, and vulnerability of European forest ecosystems. Forest Ecology and Management 259, 698–709. DOI: 10.1016/j.foreco.2009.09.023

Lobo, A., Torres-Ruiz, J.M., Burlett, R., Lemaire, C., Parise, C., Francioni, C., Truffaut, L., Tomášková, I., Hansen, J.K., Kjær, E.D., Kremer, A., Delzon, S., 2018. Assessing inter-and intraspecific variability of xylem vulnerability to embolism in oaks. Forest Ecology and Management 424, 53-61. DOI: 10.1016/j.foreco.2018.04.031

Lotfiomran, N., Köhl, M., Fromm, J., 2016. Interaction effect between elevated CO_2 and fertilization on biomass, gas exchange and C/N ratio of European beech (*Fagus sylvatica* L.). Plants 5:3, 1010-1016. DOI: 10.3390/plants5030038

Mathias, J.M., Thomas, R.B., 2021. Global tree intrinsic water use efficiency is enhanced by increased atmospheric CO_2 and modulated by climate and plant functional types. Proceedings of the National Academy of Sciences 118:7 e2014286118. DOI:10.1073/pnas.2014286118

McCarroll, D., Duffy, J.E., Loader, N.J., Young, G.H.F., Davies, D., Miles, D., Ramsey C.B., 2020. Are there enormous age-trends in stable carbon isotopes ratios of oak tree rings? The Holocene 30:11, 1637-1642. DOI: 10.1177/0959683620941073

Meier, E.S., Edwards Jr, T.C., Kienast, F., Dobbertin, M., Zimmermann, N.E., 2011. Co-occurrence patterns of trees along macro-climatic gradients and their potential influence on the present and future distribution of *Fagus sylvatica* L.: Influence of co-occurrence patterns on *Fagus sylvatica*. Journal of Biogeography 38, 371–382. DOI: 10.1111/j.1365-2699.2010.02405.x

Mérian, P., 2012. POINTER et DENDRO : deux applications sous R pour l'analyse de la réponse des arbres au climat par approche dendroécologique. Revue Forestière Française 64, 789–798.DOI: 10.4267/2042/51116

Mérian, P., Bontemps, J.D., Bergès, L., Lebourgeois, F., 2011. Spatial variation and temporal instability in climate-growth relationships of sessile oak (*Quercus petraea* [Matt.] Liebl.) under temperate conditions. Plant Ecology 212:11, 1855-1871. DOI: 10.1007/s11258-011-9959-2

Millar, C.I., Stephenson, N.L., Stephens, S.L., 2007. Climate change and forests of the future: managing in the face of uncertainty. Ecological Applications 17, 2145–2151. DOI: 10.1890/06-1715.1

Ouayjan, A., Hampe, A., 2018. Extensive sib-mating in a refugial population of beech (*Fagus sylvatica*) growing along a lowland river. Forest Ecology and Management 407, 66–74. DOI: 10.1016/j.foreco.2017.07.011

Packham, J.R., Thomas, P.A., Atkinson, M.D., Degen, T., 2012. Biological flora of the British Isles: *Fagus sylvatica*. Journal of Ecology 100, 1557-1608. DOI: 10.1111/j.1365-2745.2012.02017.x

Parmesan, C., 2006. Ecological and evolutionary responses to recent climate change. Annual Review of Ecology, Evolution, and Systematics 3, 637–669. DOI: 10.1146/annurev.ecolsys.37.091305.110100

Patterson, A.E., Arkebauer, R., Quallo, C., Heskel, M.A., Li, X., Boelman, N., Griffin, K.L., 2018. Temperature response of respiration and respiratory quotients of 16 co-occurring temperate tree species. Tree Physiology 38:9, 1319-1332. DOI: 10.1093/treephys/tpx176

Peñuelas, J., Canadell, J.G., Ogaya, R., 2011. Increased water-use efficiency during the 20th century did not translate into enhanced tree growth: Tree growth in the 20th century. Global Ecology and Biogeography 20, 597–608. DOI: 10.1111/j.1466-8238.2010.00608.x

Peñuelas, J., Hunt, J.M., Ogaya, R., Jump, A.S., 2008. Twentieth century changes of tree-ring $\delta^{13}C$ at the southern range-edge of *Fagus sylvatica*: increasing water-use efficiency does not avoid the growth decline induced by warming at low altitudes. Global Change Biology 14, 1076–1088. DOI: 10.1111/j.1365-2486.2008.01563.x

Petit, R.J., Hu, F.S., Dick, C.W., 2008. Forests of the past: a window to future changes. Science 320, 1450–1452. DOI: 10.1126/science.1155457

Phipps, R.L., 1985. Collecting, preparing, crossdating, and measuring tree increment cores. No. 85-4148. US Department of the Interior, Geological Survey

Picard, J.F., 1995. Evolution de la croissance radiale du hêtre (*Fagus sylvatica* L) dans les Vosges. Premiers résultats sur le versant lorrain. Annales Des Sciences Forestieres 52 :1, 11-21. DOI: 10.1051/forest:19950102

Piedallu, C., Perez, V., Gégout, J.C., Lebourgeois, F., Bertrand, R. 2009. Impact potentiel du changement climatique sur la distribution de l'Epicéa, du Sapin, du Hêtre et du Chêne sessile en France. Revue Forestière Française 61:6, 567-593. DOI: 10.4267/2042/32924

Piovesan, G., Biondi, F., Filippo, A.D., Alessandrini, A., Maugeri, M., 2008. Drought-driven growth reduction in old beech (*Fagus sylvatica* L.) forests of the central Apennines, Italy. Global Change Biology 14, 1265–1281. DOI: 10.1111/j.1365-2486.2008.01570.x

Piovesan, G., Di Filippo, A., Alessandrini, A., Biondi, F., Schirone, B., 2005. Structure, dynamics and dendroecology of an old-growth *Fagus* forest in the Apennines. Journal of Vegetation Science 16, 13–28. DOI: 10.1111/j.1654-1103.2005.tb02334.x

Preisler, Y., Tatarinov, F., Grünzweig, J., Bert, D., Ogée, J., Wingate, L., Rotenberg, E., Rohatyn, S., Her, N., Moshe, I., Klein, T., Yakir, D., 2019. Mortality versus survival in drought-affected Aleppo pine forest depends on the extent of rock cover and soil stoniness. Functional Ecology 33, 901-912, DOI: 10.1111/1365-2435.13302

Pretzsch, H., Schütze, G., Uhl, E., 2013. Resistance of European tree species to drought stress in mixed versus pure forests: evidence of stress release by inter-specific facilitation. Plant Biology 15, 483-495. DOI: 10.1111/j.1438-8677.2012.0 0670.x

Prislan, P., Gričar, J., Čufar, K., de Luis, M., Merela, M., Rossi, S., 2019. Growing season and radial growth predicted for *Fagus sylvatica* under climate change. Climatic Change 153:1, 181-197. DOI: 10.1007/s10584-019-02374-0

R Development Core Team., 2016. R: A Language and Environment for Statistical Computing. R Foundation for Statistical Computing, Vienna, Austria. http://www.r-project.org/

Richardson, A.D., Carbone, M.S., Keenan, T.F., 2013. Seasonal dynamics and age of stemwood nonstructural carbohydrates in temperate forest trees. New Phytologist 197: 850–861. DOI: 10.1111/nph.12042

Sánchez-Salguero, R., Camarero, J.J., Carrer, M., Gutiérrez, E., Alla, A.Q., Andreu-Hayles, L., Hevia, A., Koutavas, A., Martínez-Sancho, E., Nola, P., Papadopoulos, A., 2017. Climate extremes and predicted warming threaten Mediterranean Holocene firs forests refugia. Proceedings of the National Academy of Sciences 114:47, E10142-50. DOI: 10.1073/pnas.1708109114

Sanchez-Salguero, R., Camarero, J.J., Gutierrez, E., Gonzalez Rouco, F., Gazol, A., Sangüesa-Barreda, G., Andreu-Hayles, L., Linares, J.C., Seftigen, K., 2017. Assessing forest vulnerability to climate warming using a process-based model of tree growth: bad prospects for rear-edges. Global Change Biology 23, 2705-2719. DOI: 10.1111/gcb.13541

Stojnić, S., Suchocka, M., Benito-Garzón, M., Torres-Ruiz, J.M., Cochard, H., Bolte, A., Cocozza C., Cvjetković, B., de Luis, M., Martinez-Vilalta J., Raebild, A., Tognetti, R., Delzon, S., 2018. Variation in xylem vulnerability to embolism in European beech from geographically marginal populations. Tree Physiology 38:2, 173-185. DOI: 10.1093/treephys/tpx128

Taccoen, A., Piedallu, C, Seynave, I., Perez, V., Gégout-Petit, A., Nageleisen, L.M., Bontemps, J.D., Gégout, J.C., 2019. Background mortality drivers of European tree species: climate change matters. Proceedings of the Royal Society B-Biological Sciences. DOI: 10.1098/rspb.2019.0386

Thornthwaite, C.W., 1948. An approach toward a rational classification of climate. Geographical Review 38, 55–94

Timbal, J., Ducousso, A., 2010. Le hêtre (*Fagus sylvatica* L.) dans les Landes de Gascogne et à leur périphérie. Bulletin de La Société Linnéenne de Bordeaux 145 :38, 127–137

Timofeeva, G., Treydte, K., Bugmann, H., Rigling, A., Schaub, M., Siegwolf, R., Saurer, M., 2017. Long-term effects of drought on tree-ring growth and carbon isotope variability in Scots pine in a dry environment. Tree Physiology 37:8, 1028–1041. DOI: 10.1093/treephys/tpx041

Tognetti, R., Lombardi, F., Lasserre, B., Cherubini, P., Marchetti, M., 2014. Tree-ring stable isotopes reveal twentieth-century increases in water-use efficiency of *Fagus sylvatica* and *Nothofagus* spp. in Italian and Chilean Mountains. PloS One 9:11, e113136

Van Der Werf, G., Sass-Klaassen, U., Mohren, G., 2007. The impact of the 2003 summer drought on the intra-annual growth pattern of beech (*Fagus sylvatica* L.) and oak (*Quercus robur* L.) on a dry site in the Netherlands. Dendrochronologia 25:2, 103-112. DOI: 10.1016/j.dendro.2007.03.004

Vilà-Cabrera, A., Jump, A.S., 2019. Greater growth stability of trees in marginal habitats suggests a patchy pattern of population loss and retention in response to increased drought at the rear edge. Ecology Letters 22: 1439-1448. DOI: 10.1111/ele.13329

Voelker, S.L., Brooks, J.R., Meinzer, F.C., Anderson, R., Bader, M.K.-F., Battipaglia, G., Becklin, K.M., Beerling, D., Bert, D., Betancourt, J.L., Dawson, T.E., Domec, J.-C., Guyette, R.P., Körner, C., Leavitt, S.W., Linder, S., Marshall, J.D., Mildner, M., Ogée, J., Panyushkina, I., Plumpton, H.J., Pregitzer, K.S., Saurer, M., Smith, A.R., Siegwolf, R.T.W., Stambaugh, M.C., Talhelm, A.F., Tardif, J.C., Van de Water, P.K., Ward, J.K., Wingate, L., 2016. A dynamic leaf gas-exchange strategy is conserved in woody plants under changing ambient CO2: evidence from carbon isotope discrimination in paleo and CO2 enrichment studies. Global Change Biology 22, 889-902. DOI: 10.1111/gcb.13102

Walbott, M., 2018. Rôles des facteurs locaux dans la distribution et la persistance des communautés à hêtre (*Fagus sylvatica*) en marge d'aire de répartition. Biodiversité et Ecologie. PhD. Université de Bordeaux, 2018. Français. NNT : 2018BORD0455 . tel-02049104

Waterhouse, J.S., Switsur, V.R., Barker, A.C., Carter, A.H.C., Hemming, D.L., Loader, N.J., Robertson, I., 2004. Northern European trees show a progressively diminishing response to increasing atmospheric carbon dioxide concentrations. Quaternary Science Reviews 23, 803–810. DOI: 10.1016/j.quascirev.2003.06.011

Wigley, T.M.L., Briffa, K.R., Jones, P.D., 1984. On the average value of correlated time series, with applications in dendroclimatology and hydrometeorology. Journal of Climate and Applied Meteorology 23, 201–213

Willner, W., Jiménez-Alfaro, B., Agrillo, E., Biurrun, I., Campos, J.A., Čarni, A., Casella, L., Csiky, J., Ćušterevska, R., Didukh, Y.P., Ewald, J., Jandt, U., Jansen, F., Kącki, Z., Kavgacı, A., Lenoir, J., Marinšek, A., Onyshchenko, V., Rodwell, J.S., Schaminée, J.H.J., Šibík, J., Škvorc, Z., Svenning, J.C., Tsiripidis, I., Turtureanu, P.D., Tzonev, R., Vassilev, K., Venanzoni, R., Wohlgemuth, T., Chytrý, M., 2017. Classification of European beech forests: a gordian knot? Applied Vegetation Science 20:3, 494-512. DOI: 10.1111/avsc.12299

Wilmking, M., Maaten-Theunissen, M., Maaten, E., Scharnweber, T., Buras, A., Biermann, C., Gurskaya, M., Hallinger, M. Lange, J., Shetti, R., Smiljanic, M., Trouillier, M., 2020. Global assessment of relationships between climate and tree growth. Global Change Biology 26:6, 3212-3220. DOI: 10.1111/gcb.15057

Supporting material in the Online Appendix

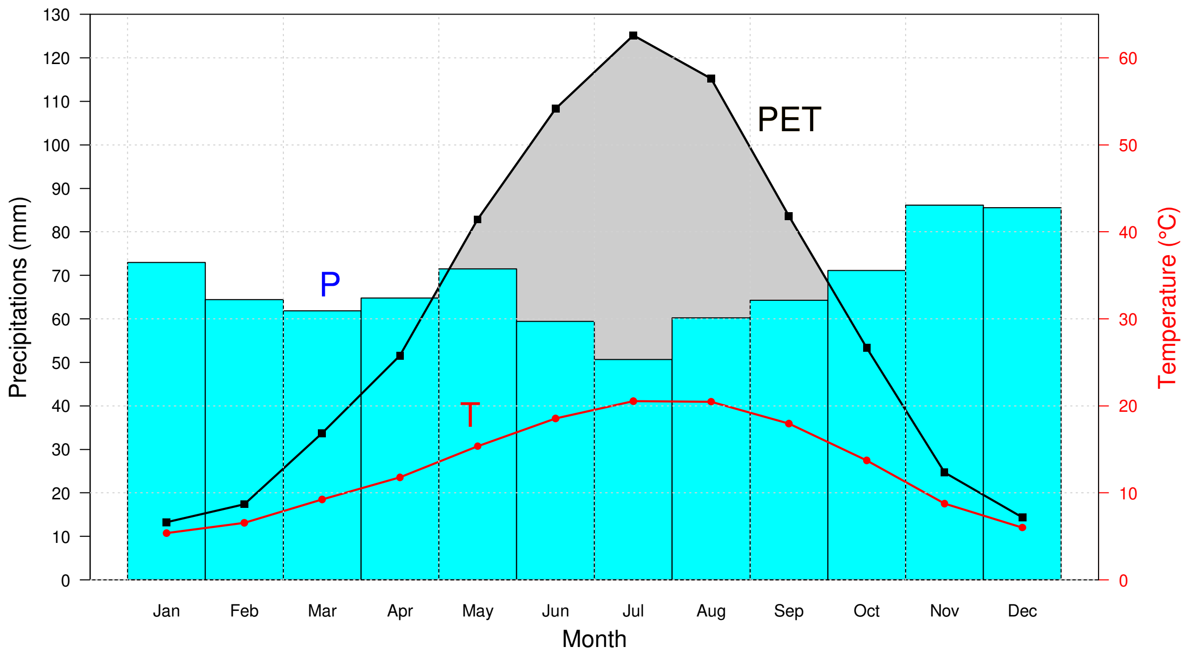

Figure S1. Climograph of the region close to the Ciron valley in the period 1897-2015 (in Sauternes). The blue bars indicate the monthly average level of precipitation (P), the red curve indicates the mean temperature (T) and the black curve indicates the mean evapotranspiration (PET). The grey area shows a deficit in climatic water balance.

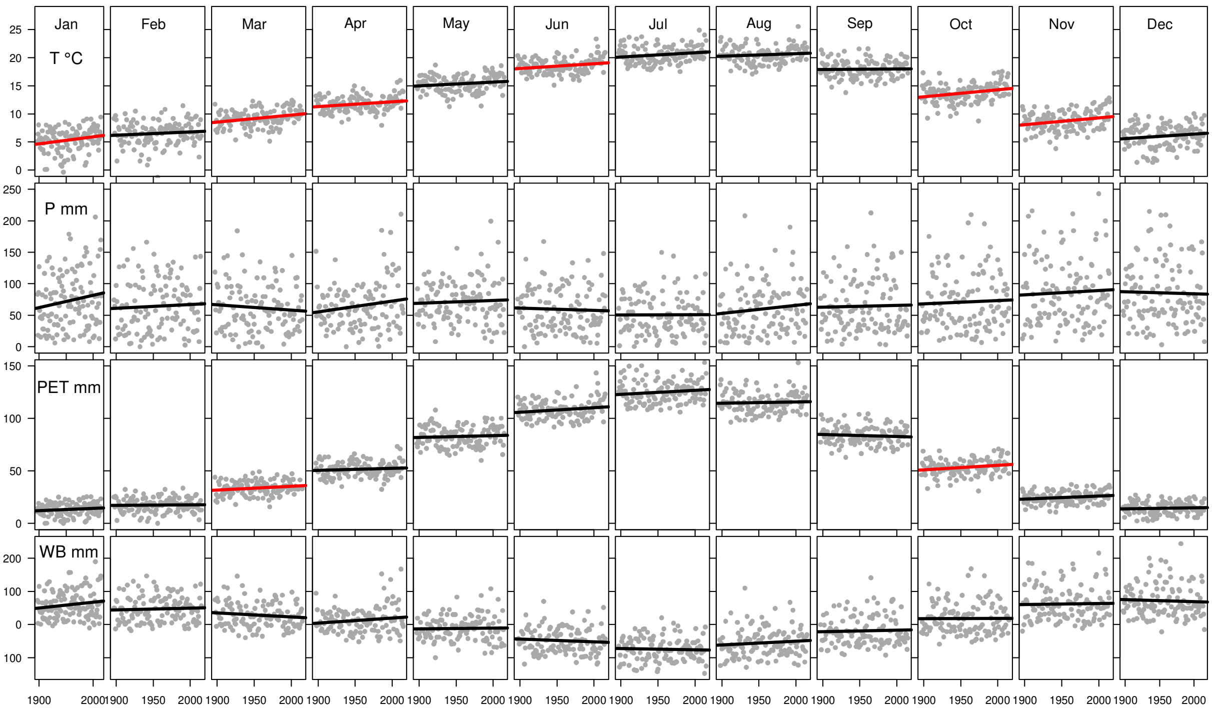

Figure S2. Mean temperature (T in °C), precipitation (P in mm), potential evapotranspiration (PET in mm), and water balance (WB in mm) for each month from 1897 to 2015. Black and red lines indicate respectively, a non-significant and a significant correlation at the 5 % threshold between the corresponding climate factor and the year.

Table S1. Pearson correlation coefficient (r), probability (pr), significance code: 0 '***' 0.001 '**' 0.01 '*' 0.05, and slope of the regression in unit per century for temperature (T) and precipitation (P) of each month from 1897 to 2015.

	Month	**Jan**	**Feb**	**Mar**	**Apr**	**May**	**Jun**	**Jul**	**Aug**	**Sep**	**Oct**	**Nov**	**Dec**
T	**r**	0.20	0.09	0.28	0.20	0.15	0.22	0.17	0.10	0.01	0.25	0.24	0.13
	pr	0.02	0.32	0.00	0.02	0.09	0.01	0.06	0.27	0.84	0.00	0.00	0.14
	Sign.	*		**	*		*				**	**	
	Slope °C/100yrs	1.24	0.59	1.24	0.82	0.67	0.88	0.75	0.44	0.01	1.28	1.23	0.81
P	**r**	0.15	0.05	-0.077	0.15	0.04	-0.035	0.00	0.11	0.02	0.04	0.04	-0.021
	pr	0.10	0.57	0.40	0.08	0.64	0.70	0.92	0.22	0.82	0.65	0.62	0.86
	Sign.												
	Slope mm/100yrs	19.5	6.2	-8.4	17.2	4.1	-3.5	0.3	12.8	2.5	5.2	6.7	-3.1

Table S2. Potential Evapotranspiration calculated with Thornthwaite method and climatic water balance

From minimal and maximal temperature per day (°C) and rain rate per day (mm) we derived the following variables over the period 1897–2015: annual mean temperature, monthly mean temperature, total annual precipitation, monthly precipitation, annual and monthly potential evapotranspiration (PET) using the Thornthwaite method (Thornthwaite, 1948), and monthly and annual climatic water balance (WB).

$$PET = 16\,D\left(\frac{(10\,T_m)}{I}\right)^a$$

with PET: the monthly potential evapotranspiration in mm,

T_m: the mean monthly temperature (°C),

I: sum over 12 months of $\left(\frac{T_m}{5}\right)^{1.514}$

$a = 0.49239 + 1.792\;10^{-2}\,I + 7.71\;10^{-5}\,I^2 + 6.75\;10^{-7}\,I^3$

D: coefficient that represents the mean possible duration of sunlight that differs from month to month and according to latitude (Thornthwaite, 1948). In the Ciron valley (44° N), $D_{January}$ = 0.81; $D_{February}$ = 0.82; D_{March} = 1.02; D_{April} = 1.13; D_{May} = 1.27; D_{June} = 1.29; D_{July} = 1.3; D_{August} = 1.2; $D_{Septembre}$ = 1.04; $D_{Octobre}$ = 0.95; $D_{Novembre}$ = 0.8 and $D_{Decembre}$ = 0.76.

$$WB = P - PET$$

with WB: monthly climatic water balance in mm,

P: mean monthly precipitation in mm,

PET: monthly potential evapotranspiration in mm.

Table S3. Summary of the main steps linking carbon stable-isotopes composition and intrinsic water-use efficiency.

The isotopic composition of a carbon compound $\delta^{13}C$ is the proportional deviation of the $^{13}C/^{12}C$ ratio from the internationally accepted Peedee belemnite (PDB) carbonate standard (Craig, 1957):

Eq 1 $$\delta^{13}C\ (‰) = \left(\frac{(^{12}C/^{13}C)_{sample}}{(^{12}C/^{13}C)_{PDB}} - 1\right) 1000 = \delta_{plant}$$

During carbon fixation, some fractionations associated with physical and enzymatic processes lead organic matter in plant to be ^{13}C depleted in comparison with the air. The $\delta^{13}C$ of atmospheric CO_2, δ_a, has a current value of about -8.5‰ and plant material δ_{plant} ranges from -22‰ to -34‰. The carbon isotopic discrimination is expressed as

Eq 2 $$\Delta\ (‰) = \frac{\delta_a - \delta_{plant}}{1 + \delta_{plant}}$$

The relative rates of CO_2 diffusion, via stomata, into the leaf and its fixation by ribulose-1,5 bisphosphate carboxylase/oxygenase (RuBisCO) are the primary factors determining Δ. According to the model proposed by Farquhar et al. (1982):

Eq 3 $$\Delta\ (‰) = a + (b - a)\frac{C_i}{C_a} - d \quad \rightarrow \quad C_i = C_a\left(\frac{\Delta - a + d}{b - a}\right)$$

where a is the discrimination against $^{13}CO_2$ during CO_2 diffusion through the stomata (a = 4.4‰, O'Leary, 1981), b is the discrimination associated with carboxylation by RuBisCO (b = 27‰, Farquhar and Richards, 1984), d is a term related to a variety of factors (respiration, liquid-phase diffusion, etc.), often taken as a constant of 1‰, and C_i and C_a are intercellular and ambient CO_2 concentrations.

Given Fick's law, $A = g_{CO2}\ (C_a - C_i)$

where A, the net photosynthesis measured as CO_2 uptake, and g_{CO2} leaf conductance to CO_2, are linked, and given that g_{H2O}, the leaf conductance to water vapour is 1.6 (g_{CO2}), Δ can be related to the ratio A/g_{H2O} by

Eq 4 $$\Delta(‰) = a - d + (b - a)\left(1 - \frac{1.6}{C_a}\frac{A}{g_{H_2O}}\right)$$

A/g_{H2O} is called intrinsic Water Use Efficiency (iWUE) (Ehleringer et al., 1993), which is a component of plant transpiration efficiency, the long-term expression of biomass gain with respect to water loss at the level of the whole plant. Finally, according to the last formula the instantaneous iWUE is expressed as the following,

Eq 5 $$\frac{A}{g_{H_2O}} = \frac{C_a}{1.6}\left(1 - \frac{\Delta - a + d}{b - a}\right) = iWUE$$

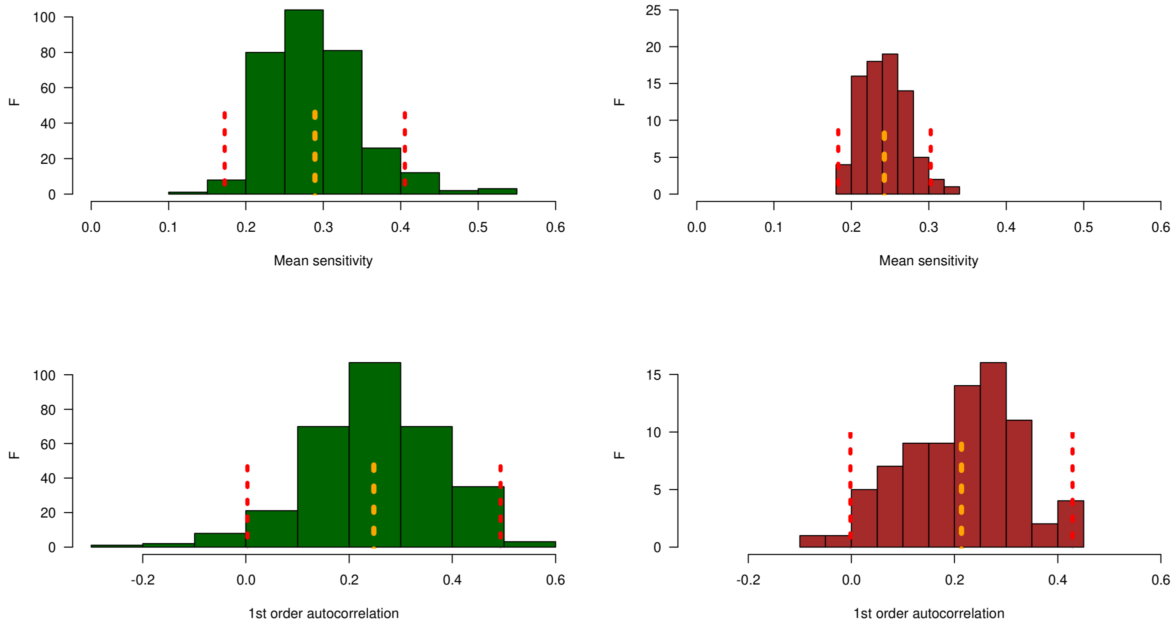

Figure S3. Distribution of mean sensitivity and first order correlation in the population of *Fagus* (green) and *Quercus* (brown). The orange dotted line displays the mean and the 95 % confidence interval of the mean is delimited by two red dotted lines. For each individual within a population, the mean sensitivity (MS) measures the year-to-year variability and expresses the extent of the short-term changes affecting the tree-ring width; it varies between 0 to 2. The average MS value was 0.289 for *Fagus* and 0.243 for *Quercus* (Table 1) which is in the range of usual values in natural forests; the variability showed that some trees were more sensitive than others. On each series, the first-order correlation (Ar1) estimates the interdependence between two successive rings of the same time series, i.e. it quantifies the effect of persistence related to the conditions leading to the development of the ring of the year (t-1) on the development of the ring of the following year (t). On double-spline detrended series of RW, the average value of AR was 0.248 for *Fagus* and 0.213 for *Quercus*. 58 % and 61 % of the values were significant at the 5 % threshold for *Fagus* and *Quercus*, respectively. These correlations show that some variations of growth follow a pattern with lower growth during few years (Fig.3, e.g in the 1940s), followed by few years with higher growth (e.g in the 1950s) etc. The interannual variations of *Fagus* and *Quercus* are also marked and the trees decrease and recover fast their growth rate. The simultaneity of such variations at the population level are consistent with climatic effects.

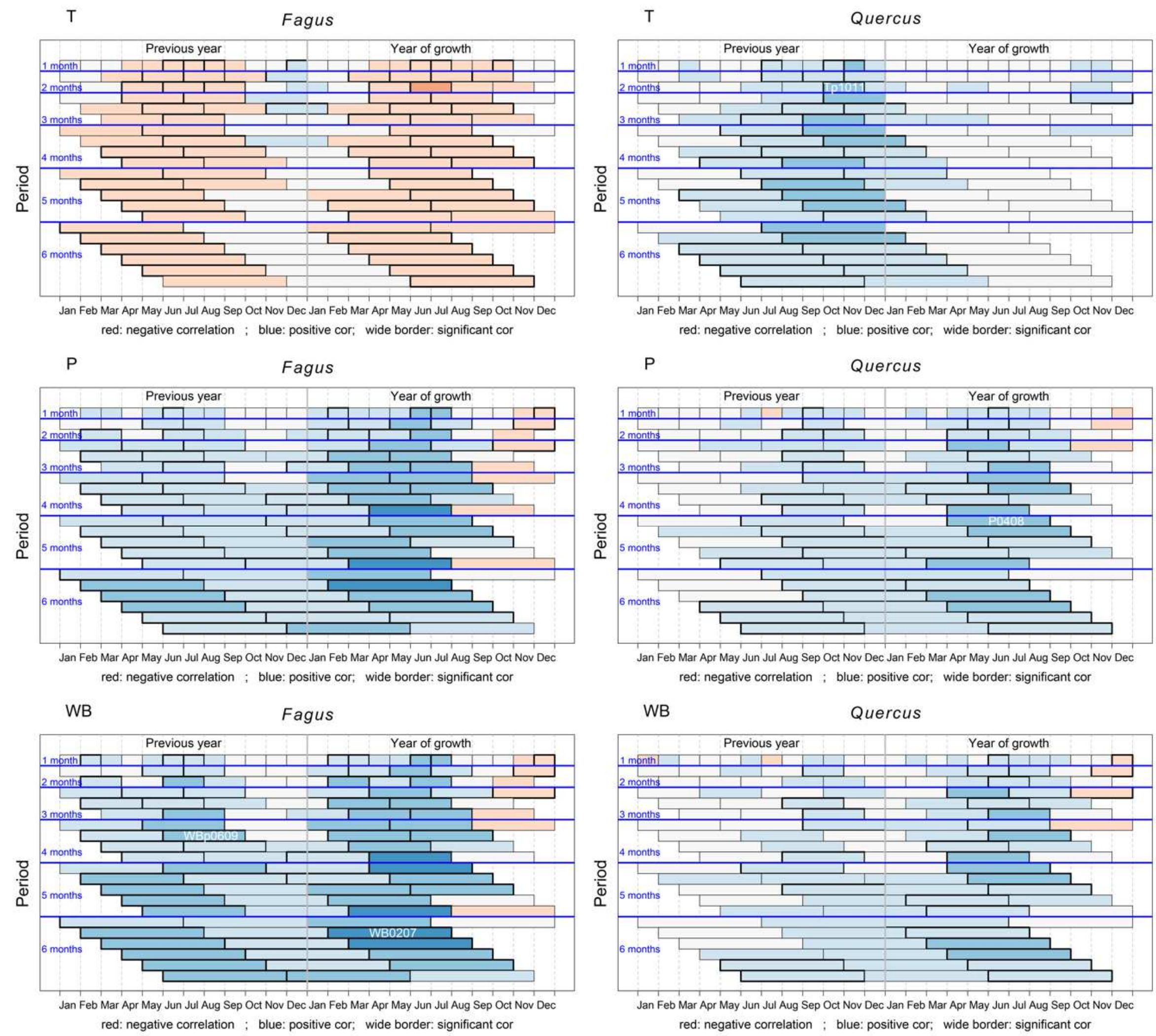

Figure S4. BCC for previous and current months (X-axis), period of time (Y-axis), climatic variable (3 rows: temperature T, precipitation P, and climatic water balance WB) and species (2 columns). The red colour displays the negative correlations between radial growth and climate, the blue colour is for positive correlations and white for BCC around zero. The intensity of the colour indicates the value of BCC: red for negative values, and blue for positive ones. Significant BCC are indicated by a larger frame. The names of the variables in the climatic models are written in white.